NASA TN D-415

NASA TN D-415

7N-02
199047
36P.

TECHNICAL NOTE
D-415

AN EXPERIMENTAL INVESTIGATION OF THE EFFECT OF WIND TUNNEL WALLS ON THE AERODYNAMIC PERFORMANCE OF A HELICOPTER ROTOR

By Victor M. Ganzer and William H. Rae, Jr.

University of Washington

NATIONAL AERONAUTICS AND SPACE ADMINISTRATION

WASHINGTON May 1960

1S

NATIONAL AERONAUTICS AND SPACE ADMINISTRATION

TECHNICAL NOTE D-415

AN EXPERIMENTAL INVESTIGATION OF THE EFFECT OF WIND TUNNEL WALLS ON THE AERODYNAMIC PERFORMANCE OF A HELICOPTER ROTOR

By

Victor M. Ganzer
and
William H. Rae, Jr.

D
4
1
5

SUMMARY

The purpose of this test was to determine, experimentally, the range of advance ratio and blade angle in which wind tunnel wall corrections as developed for wings might be used for helicopter rotors.

A three foot diameter, two bladed rotor was tested in the University of Washington 8 ft. by 12 ft. tunnel, and in 3 by 4.5 ft. and 2.4 by 3.6 ft. cross section inserts within the main tunnel.

Lift and drag coefficient data were corrected by standard wing type wall corrections using the full span of the rotor as the vortex span and the area of the rotor disc as the wing area.

Data from the three test section sizes were compared to determine at which blade angles and advance ratios the wind tunnel wall correc tions gave satisfactory agreement.

It was found that standard wind tunnel wall corrections gave satis-factory agreement at advance ratios above 0.10. At the advance ratio of 0.10, reasonable agreement occurred at a blade angle of -3.9 deg., corresponding to lift coefficients of less than 0.5, but agreement at higher blade angles was unsatisfactory.

INTRODUCTION

Very little information exists on the effect of wind tunnel walls on the aerodynamic performance of helicopters. The purpose of this investigation was to attempt to obtain experimental data on this subject which might result in useful wind tunnel wall corrections.

Standard methods for obtaining the effects of wind tunnel walls experimentally are to test a model in wind tunnels of different size, or to test similar models of different size in the same tunnel. The results are then compared, using the best theory available, and if the results of all of the tests with various ratios of model to tunnel size agree, this theory is accepted as being useful.

The method used in this test was that of using a single model in tunnels of different size. These tunnels, except for the largest tunnel, were obtained by placing inserts within the main tunnel. Although this method has shortcomings because of the finite length of the inserts, it was accepted because it was much more simple to construct and provide power for a single rotor than to do so for several rotors of different size. Further, Reynolds number proved to be quite critical in this test, and it was felt wise to have a single rotor size with the attendant constant Reynolds number in each size test section.

The tests were conducted in the University of Washington 8 ft. by 12 ft., 250 MPH wind tunnel, and were sponsored by the National Advisory Committee for Aeronautics.

SYMBOLS AND DEFINITIONS

$C_L = \frac{L}{q\,s}$	Lift coefficient
$C_D = \frac{D}{q\,s}$	Drag Coefficient
L	Lift force, perpendicular to free stream direction, lb
D	Drag force, parallel to free stream direction, lb
$q = 1/2\,\rho v^2$	Dynamic pressure, lb/sq. ft.

S	Area of disc swept by rotor blades, sq. ft.
α	Angle of attack of a plane perpendicular to the rotor shaft angle. (see fig. 1)
Blade Angle	Angle between blade chord and a plane perpendicular to rotor shaft when blades are in this plane. (see fig. 1)
Advance ratio	$\frac{\text{free stream velocity}}{\text{(rotor angular velocity) (radius of blade)}}$

APPARATUS

The University of Washington wind tunnel (fig. 2) is of the double-return type, has an 8 ft. x 12 ft. test section, and has a top speed of 250 MPH. Forces from the model are transferred through a single strut to a mechanical-electrical balance which measures six components about the tunnel centerline. A description of the tunnel may be found in ref. 1.

The model consisted of a two bladed rotor three feet in diameter. The 3'' chord blades had Rhodes St. Genese 35 airfoil sections. Drawings and photographs of the model are shown in fig. 3 and photos 1 and 2. The rotor blades were made of laminated mahogany leading edges and balsa trailing edges cemented to a steel, tubular spar, and covered with silkspan and doped. The blades were hinged at the root to allow for flapping and in-plane bending; the in-plane bending hinges were equipped with rubber dampers.

The rotor was driven by a 20 HP A. C. motor which was mounted directly below the rotor on the support strut as shown in photo 1. The entire strut, motor, and pitch-angle-change mechanism was enclosed in a streamlined windshield with a 28 inch chord and a thickness of 5.26 inches as shown in photo 3. The rotor, which was mounted on the centerline of the tunnel, pitched about a pivot 10.3'' below the rotor.

Two tunnel inserts, one 3.0 x 4.5 ft. in cross section by 8 ft. long, the other 2.4 x 3.6 ft. in cross section by 8 ft. long, were mounted in the test section as shown in photos 4 to 8. The rotor was installed 3 ft. from the leading edges of the inserts along the insert centerline.

The inserts were constructed of 1/2'' plywood. A series of static pressure orfices was installed in the sidewalls of each insert for use in velocity calibration.

TESTS AND RESULTS

A summary of the range of test variables reported herein is contained in the table I.

Results are plotted with and without wind tunnel wall corrections in figures 4 to 13. Plotted are drag polars and lift curves for various test section sizes and tip speed ratios.

The data were reduced and corrections applied as indicated in the following summary.

1. The data, which were taken at constant α , were plotted against advance ratio, and values of lift and drag were picked off of these plots at various constant advance ratios, where advance ratio was defined as

$$\text{advance ratio} = \frac{\text{free stream velocity}}{\text{(rotor angular velocity) (rotor radius)}}$$

This procedure was necessary because it was difficult to test at constant advance ratio because of the effect of power input to the rotor on the velocity calibration. Uncorrected values of the free stream dynamic pressure with inserts installed were obtained from a total pressure tube built into the rotor fairing and the static pressures from a point near the leading edge of the walls with the rotor removed. Since the wall static pressures were less than one diameter ahead of the rotor centerline, the local static pressure field of the rotor affected the wall statics. This effect was complicated by the fact that the energy added to the air stream by the rotor also affected the wall statics. The dynamic pressures were approximately corrected for the effect of the pressure field due to the rotor.

With no inserts the standard wind tunnel system was used to obtain dynamic pressure, and no corrections for the static pressure field due to the rotor were deemed necessary.

2. Forces were reduced to lift and drag coefficients by the formulas $C_L = \frac{L}{q\ s}$ and $C_D = \frac{D}{q\ s}$, where L and D were lift and drag from step 1, S was the area swept by the rotor disc, 7.07 sq. ft., and q was obtained as indicated previously.

3. Upflow angles were obtained from tests of a three foot span, 6 inch chord wing with a symmetrical section, which was placed in the position of the rotor in each insert. The drag and rotor shaft angle corrections due to upflow were of the form

$$\Delta\alpha_u^{\circ}, \text{ upflow, deg.} \quad \text{or } \Delta\alpha_u^{R}, \text{ upflow, rad.}$$

$$C_D = (\Delta\alpha_u^{R})\ (C_L)$$

and were applied to all data, thus giving data correct except for wind tunnel wall corrections.

4. Wind tunnel wall corrections were applied based on the area of a round wing 3 ft. in diameter and a vortex span of 3 ft. These corrections were of the standard form of

$$\Delta\alpha^{\circ} = \frac{S}{C}\ C_L\ (57.3)$$

$$C_D = \delta \frac{S}{C}\ C_L^{\ 2}$$

where δ was the wall correction factor, and C was the cross sectional area of the test section. Thus, the data entirely corrected were as follows

$$C_L = C_{L\ \text{measured}}$$

$$\alpha = \alpha_{\text{geometric}} + \Delta\alpha_u^{\circ} + \delta \frac{S}{C}\ C_L\ (57.3)$$

$$C_D = C_{D\ \text{measured}} + (\Delta\alpha_u^{R})\ (C_L) + \delta \frac{S}{C}\ C_L^{\ 2}$$

Valves used in the above corrections were

Test Section	δ	C	S
8.0 x 12.0 ft.	.118	96 sq. ft.	7.07 sq. ft.
3.0 x 4.5 ft.	.110	13.5	7.07
2.4 x 3.6 ft.	.115	8.64	7.07

The coefficients thus obtained are plotted with and without wall corrections in figures 4 to 13.

D
4
1
5

DISCUSSION

In the early phases of this experiment it was hoped that the data would be sufficiently consistent so that values of wind tunnel wall corrections could be derived from the data. However, it soon became apparent that the data from the test were not sufficiently precise to allow this, and it was decided to compare the data using standard wind tunnel corrections as applied to wings.

The lack of precision was the result of several causes, some of which were: forces too small compared to the capacity of the balances; uncertain dynamic pressure measurements due to inability of reading the manometer closer than 0.05'', and approximations made in correcting for the pressure field of the rotor; uncertain flow conditions on the rotor blades due to the sensitive Reynolds number range in which they were operating.

Several runs were made to check repeatability, and these showed that the lift coefficients repeated to within 0.02 at an advance ratio of 0.10, and to 0.005 at an advance ratio of 0.30. The corresponding drag coefficient increments were about 0.005 and 0.000.

It was felt that the data were sufficiently consistent to show polar shapes and lift curve slopes, and since these are the items affected by wind tunnel wall corrections, it was decided to compare the data with standard wall corrections.

The results show that standard wind tunnel wall corrections may be used for helicopter rotors, using the swept area of the disc as the reference area, with a reasonable degree of confidence, particularly at large values of the advance ratio. At the lowest value of advance ratio tested, 0.10, (fig. 4) such corrections seem reliable at low lift coefficients but at blade angles corresponding to lift coefficients above one the agreement between results from the various test sections using standard wall corrections was not satisfactory. This might indicate that this advance ratio of 0.10 was near the lower limit of the satisfactory use of such wall corrections.

CONCLUSIONS

It may be concluded that the use of standard wind tunnel wall corrections for helicopter tests should prove satisfactory, especially at advance ratios above 0.1. Such wall corrections should be based on the swept area of the rotor disc.

D
4
1
5

University of Washington
College of Engineering
Department of Aeronautical Engineering
Seattle, Washington
January 18, 1960

REFERENCE

1. Kirsten, Frederick K., and Eastman, Fred S.: The University of Washington's New 250 m.p.h. 8x12 Foot Wind Tunnel. Jour. Aero. Sci., vol. 6, no. 12, Oct. 1959, pp. 494-498.

TABLE I

SUMMARY OF VARIABLES TESTED

Test Section or Insert Cross Section	Blade Angle at Advance Ratio of				
	0.10	0.15	0.20	0.25	0.30
8.0 x 12.0 ft.	-3.9^{o}, -1^{o}, $+1.9^{o}$	-3.9^{o}, -1^{o}, $+1.9^{o}$	-3.9^{o}, -1^{o}	-3.9^{o}, -1^{o}	-3.9^{o}, -1^{o}
3.0 x 4.5 ft.	-3.9^{o}, -1^{o}, $+1.9^{o}$	-3.9^{o}, -1^{o}, $+1.9^{o}$	-3.9^{o}, -1^{o}	-3.9^{o}, -1^{o}	-3.9^{o}, -1^{o}
2.4 x 3.6 ft.	-3.9^{o}, -1^{o}	-3.9^{o}, -1^{o}	-3.9^{o}, -1^{o}	-3.9^{o}, -1^{o}	-3.9^{o}, -1^{o}

D415

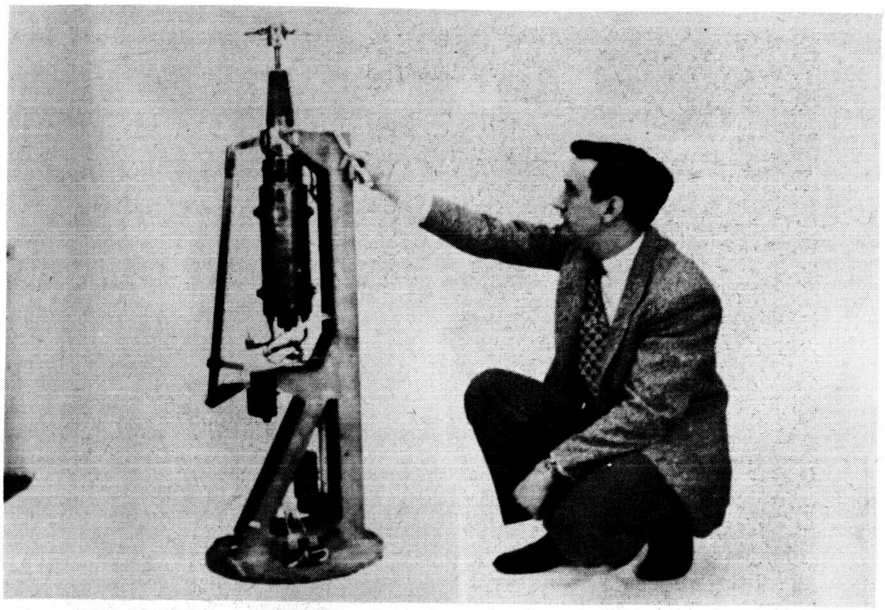

Photo 1.
Rotor Mounted on Support Strut

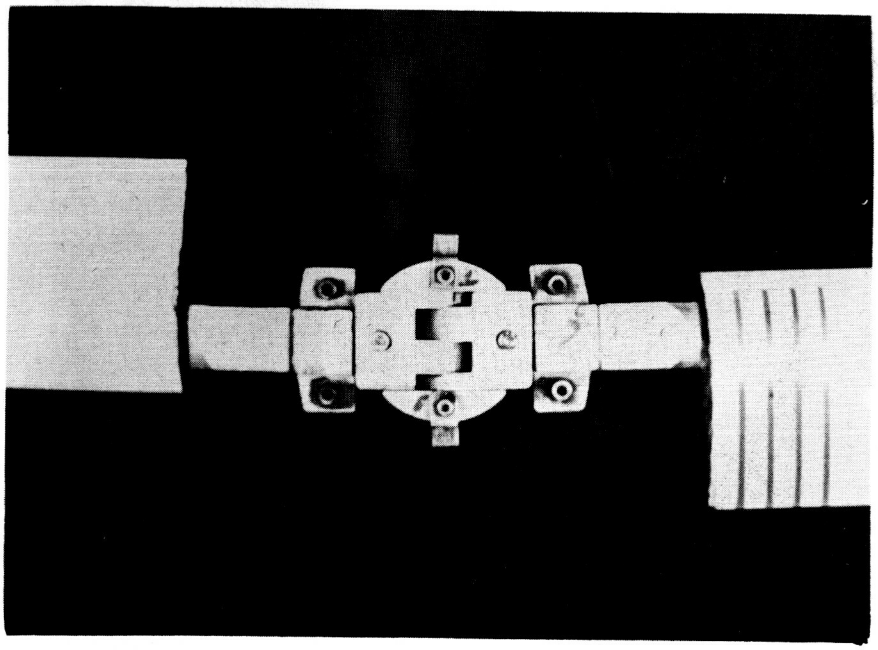

Photo 2.
Rotor Assembly

L-60-294

D-415

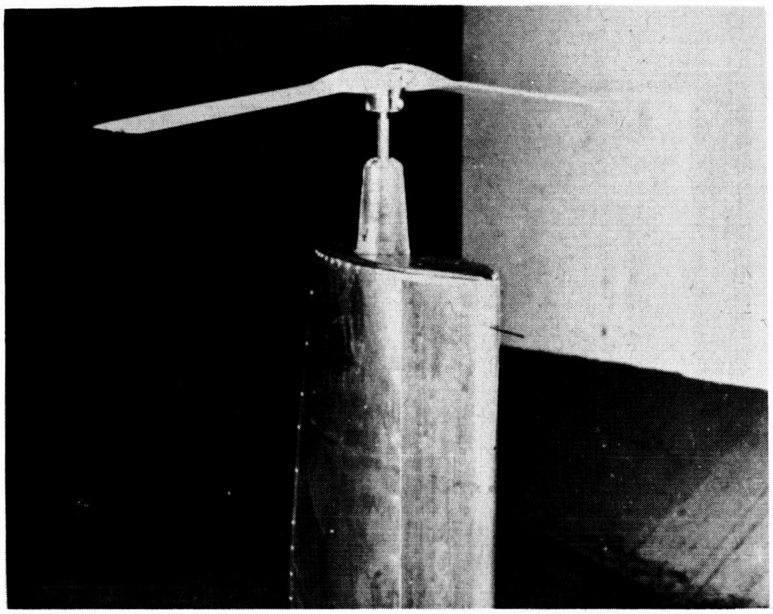

Photo 3.
Rotor Installed in 8.0 x 12.0 ft. Test Section

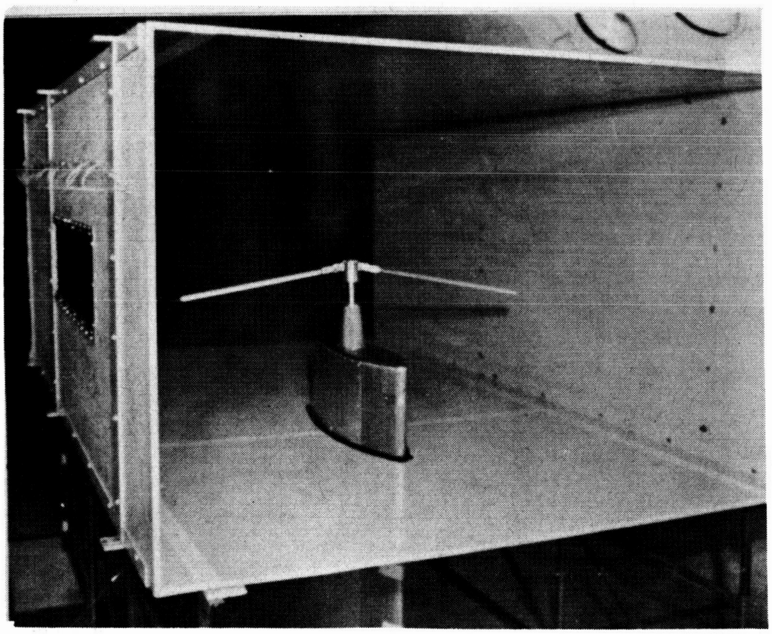

Photo 4. L-60-295
Rotor Installed in 3.0 x 4.5 ft. Insert

D-415

D-415

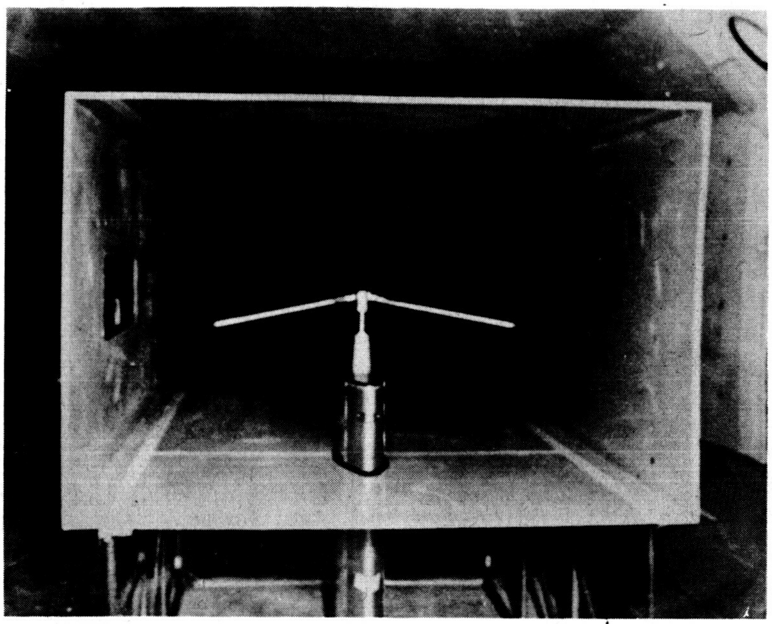

Photo 5.
Rotor Installed in 3.0 x 4.5 ft. Insert. Front View

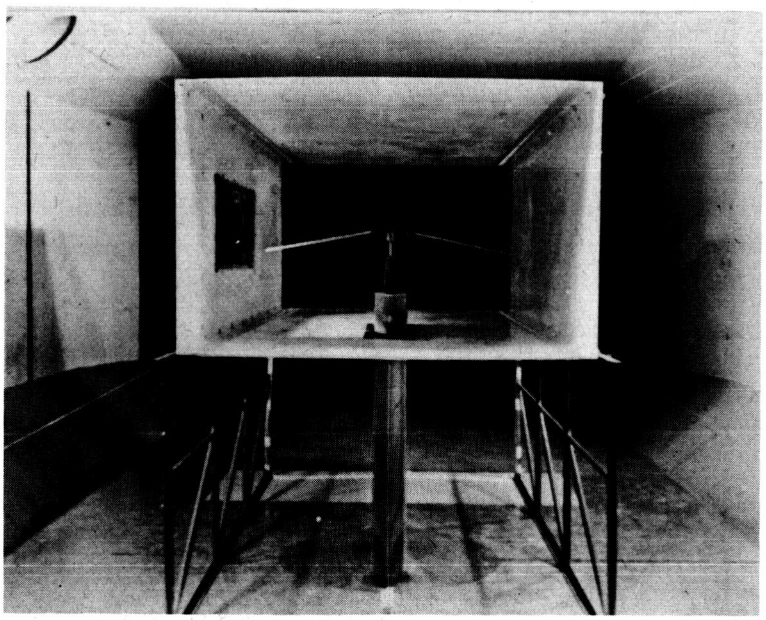

Photo 6. L-60-296
Rotor Installed in 2.4 x 3.6 ft. Insert. Front View

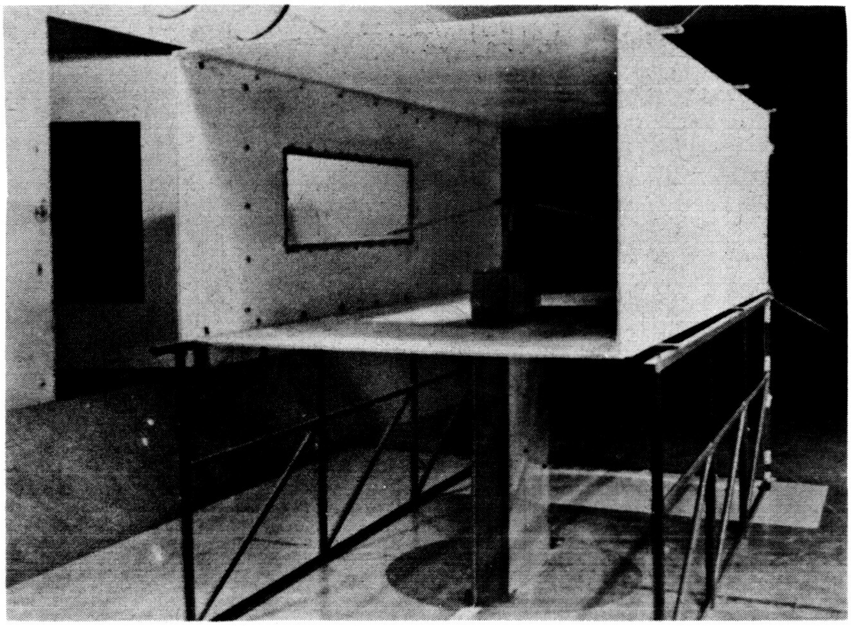

Photo 7.
Rotor Installed in 2.4 x 3.6 ft. Insert

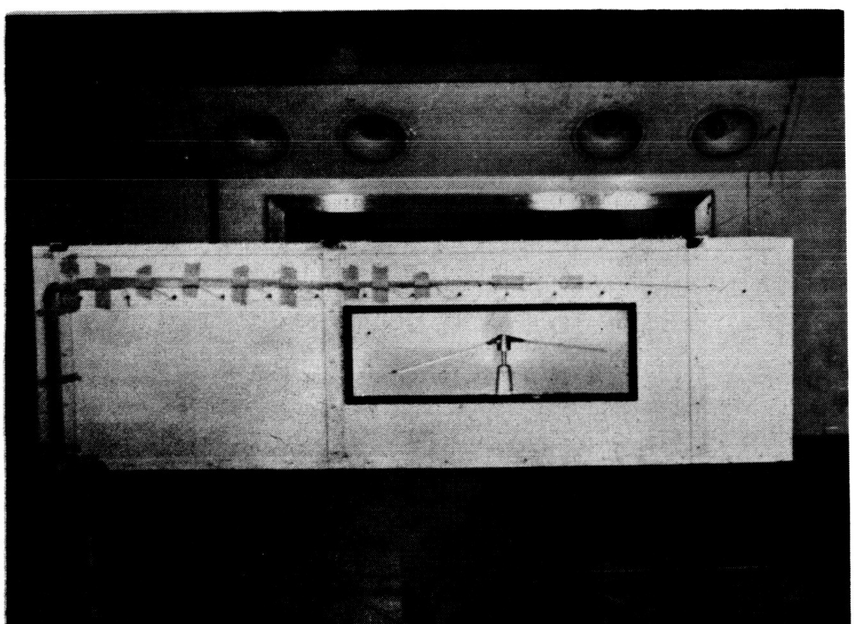

Photo 8. L-60-297
Rotor Installed in 2.4 x 3.6 ft. Insert. Side View

D-415

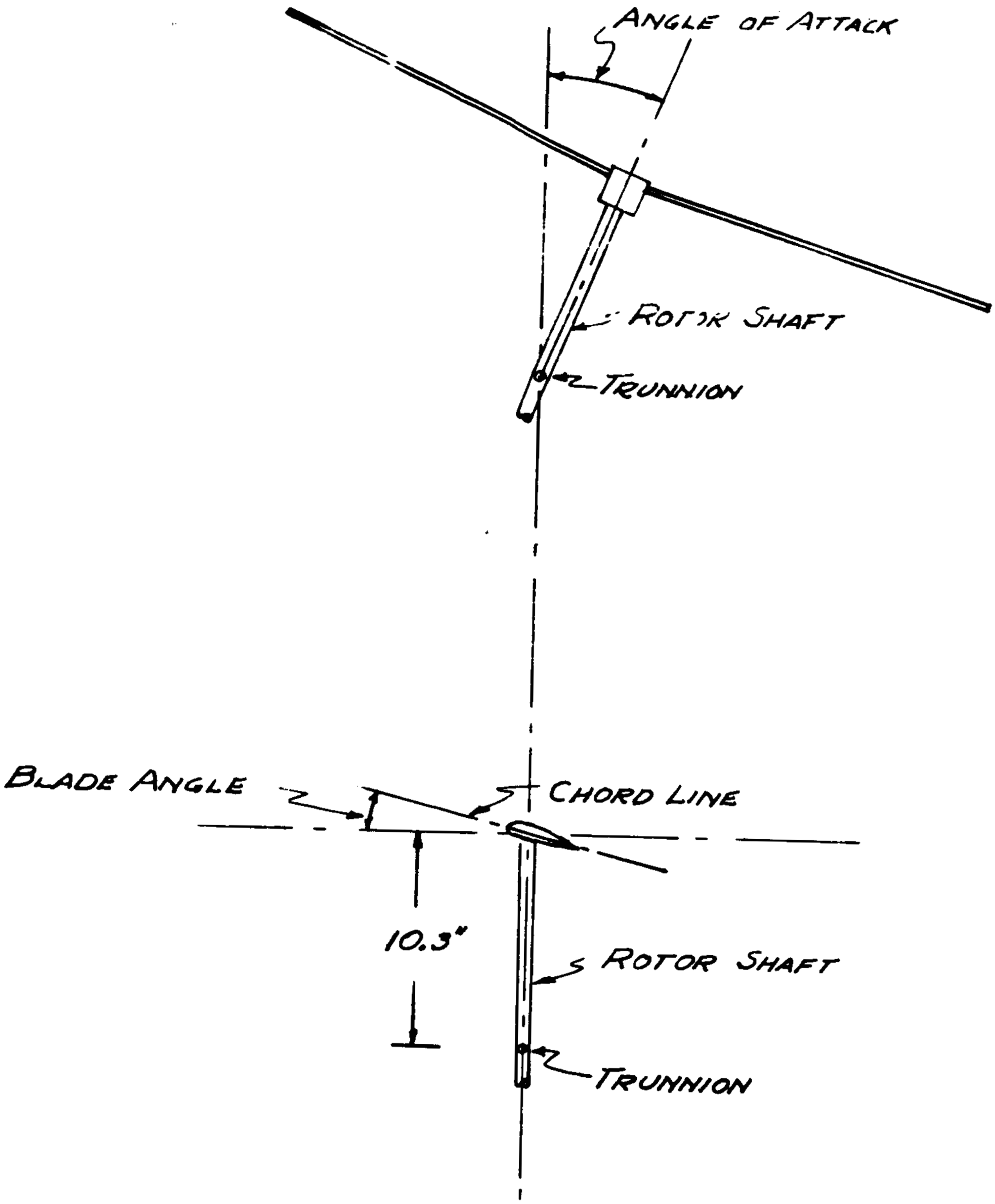

FIG. 1
DEFINITION OF ANGLES

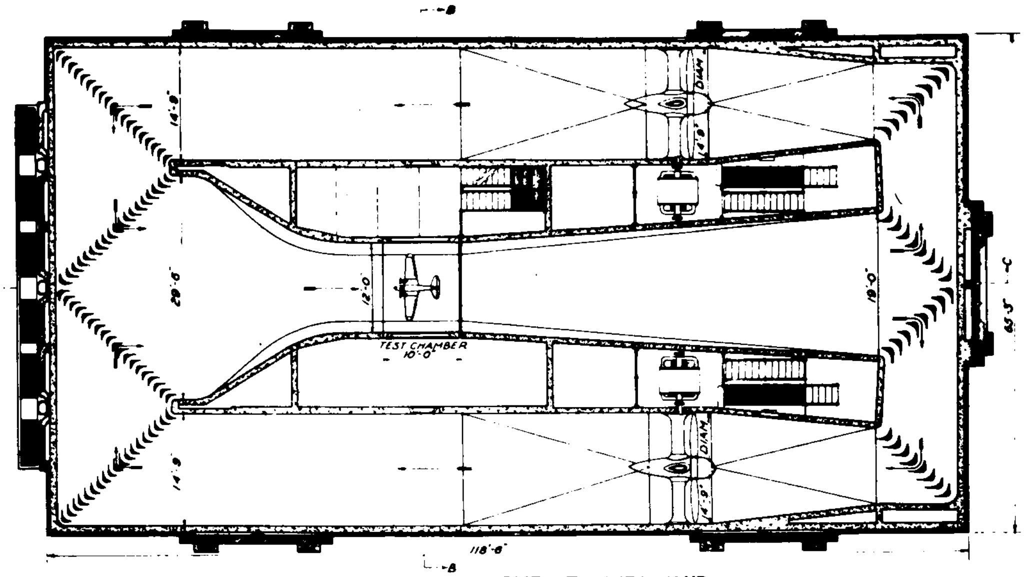

SECTIONAL PLAN THRU TUNNEL AXIS

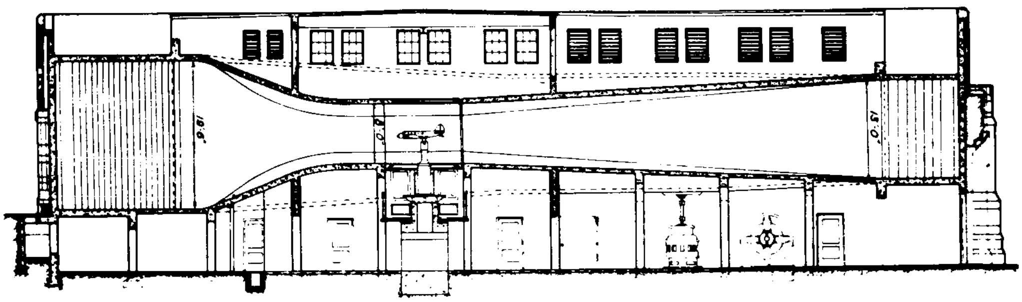

SECTIONAL ELEVATION "C"

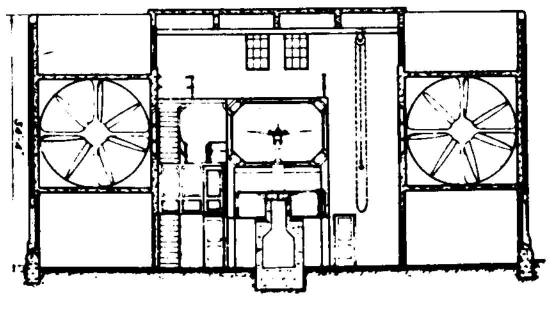

SECTIONAL ELEVATION "B"

FIG. 2
UNIVERSITY OF WASHINGTON — 250 MPH WIND TUNNEL

D-415

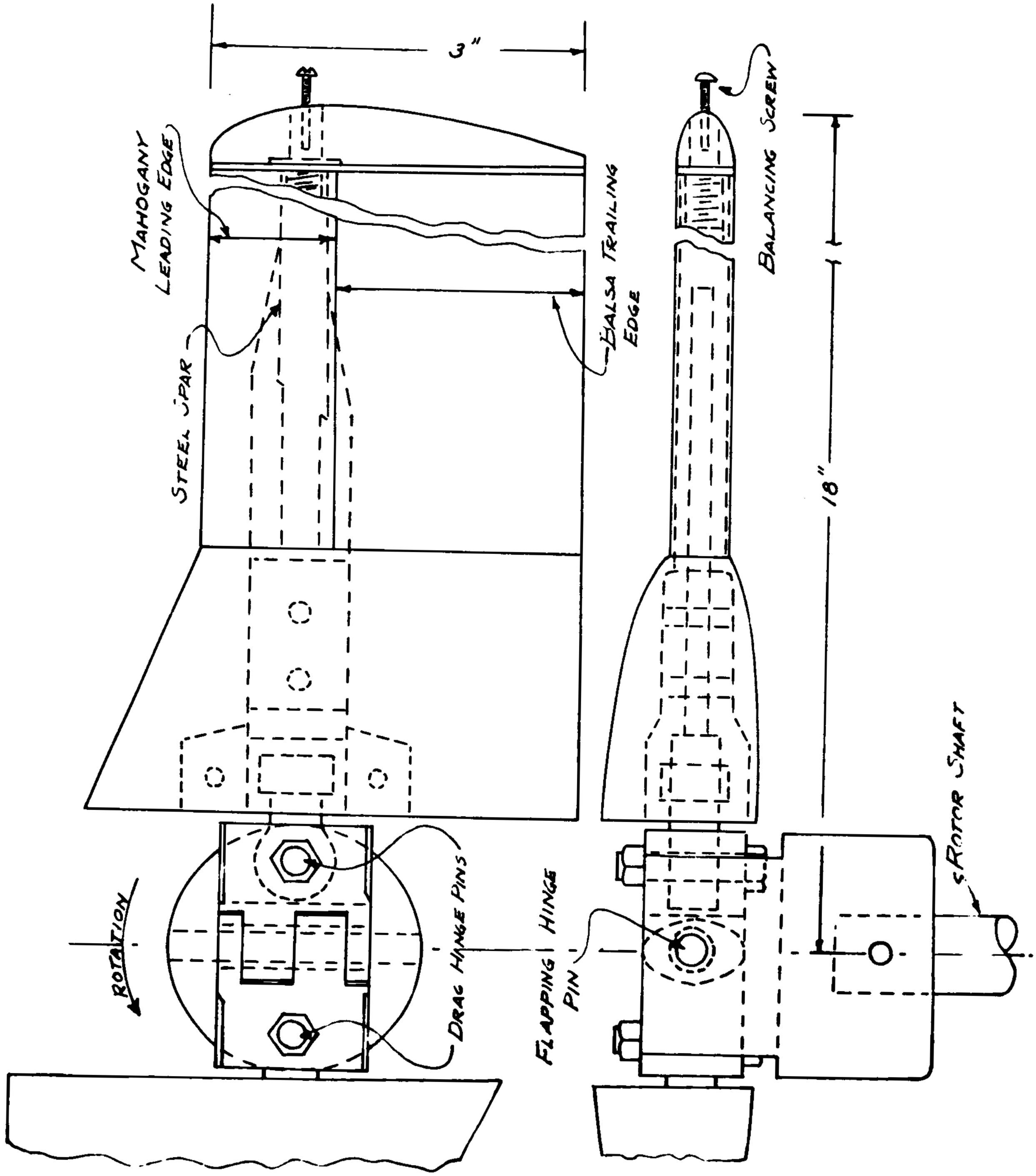

Fig. 3
Assembly Sketch of Rotor

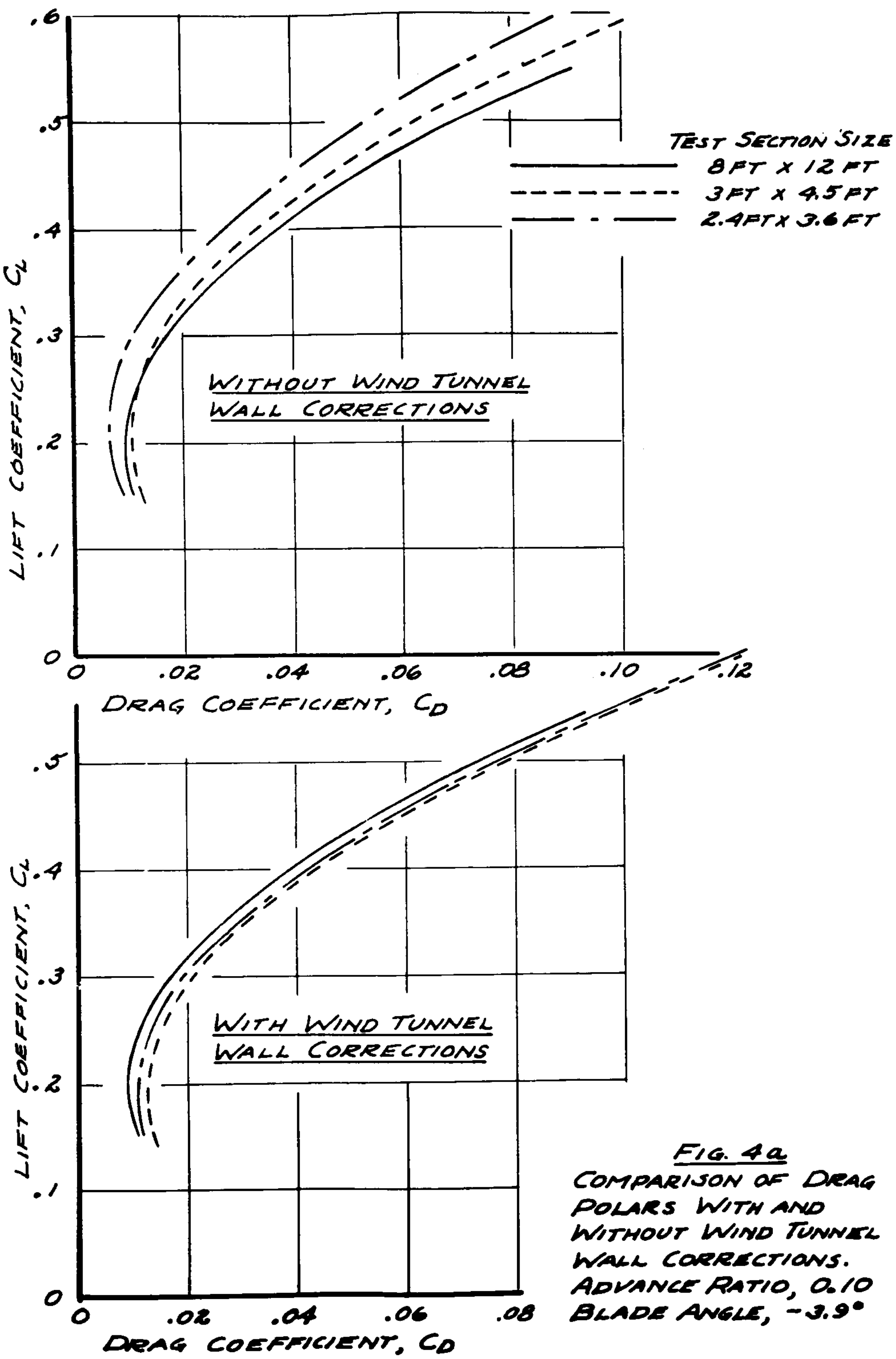

FIG. 4a
COMPARISON OF DRAG POLARS WITH AND WITHOUT WIND TUNNEL WALL CORRECTIONS.
ADVANCE RATIO, 0.10
BLADE ANGLE, −3.9°

D-415

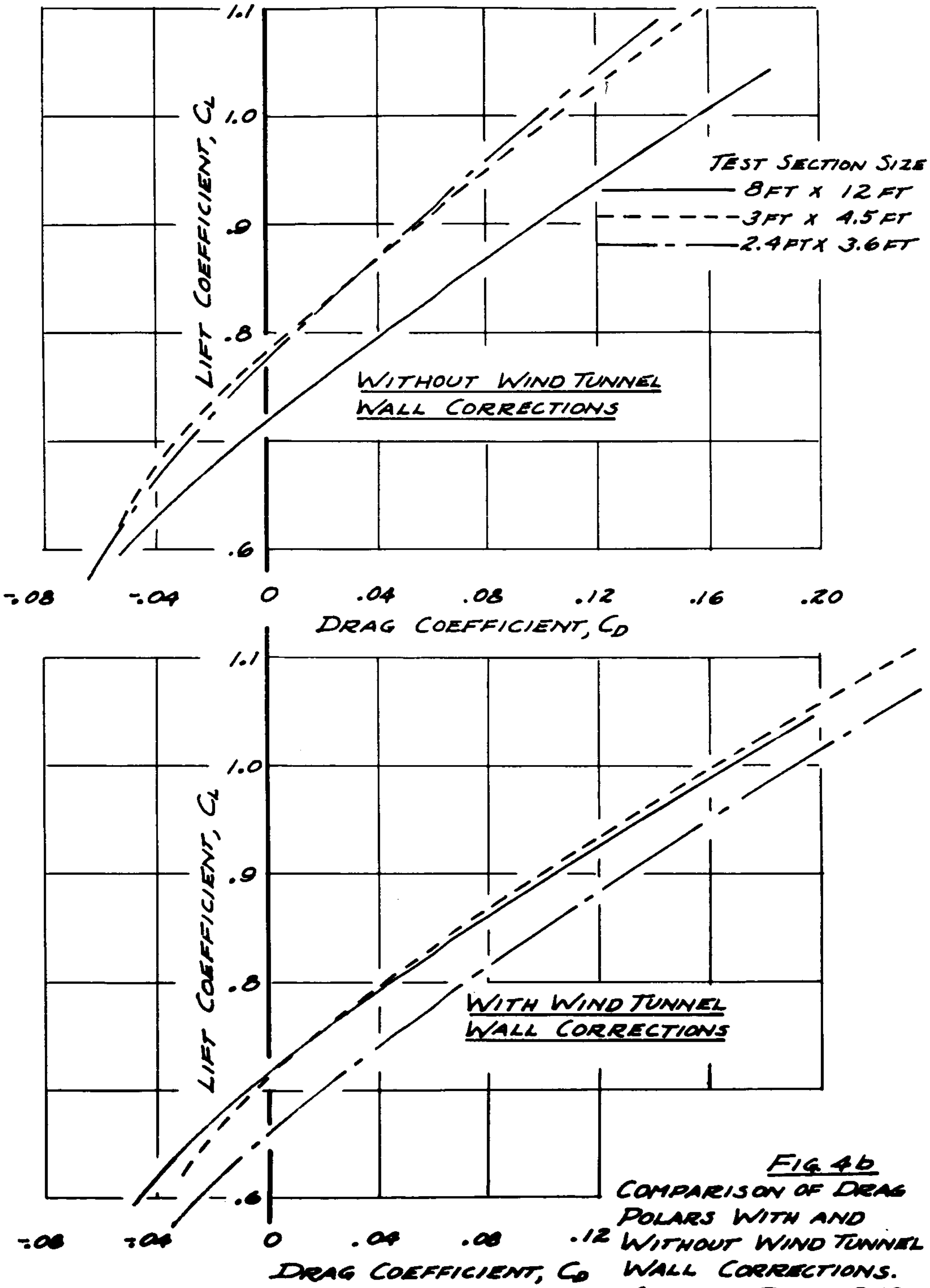

FIG. 4b
COMPARISON OF DRAG POLARS WITH AND WITHOUT WIND TUNNEL WALL CORRECTIONS.
ADVANCE RATIO, 0.10
BLADE ANGLE, -1°

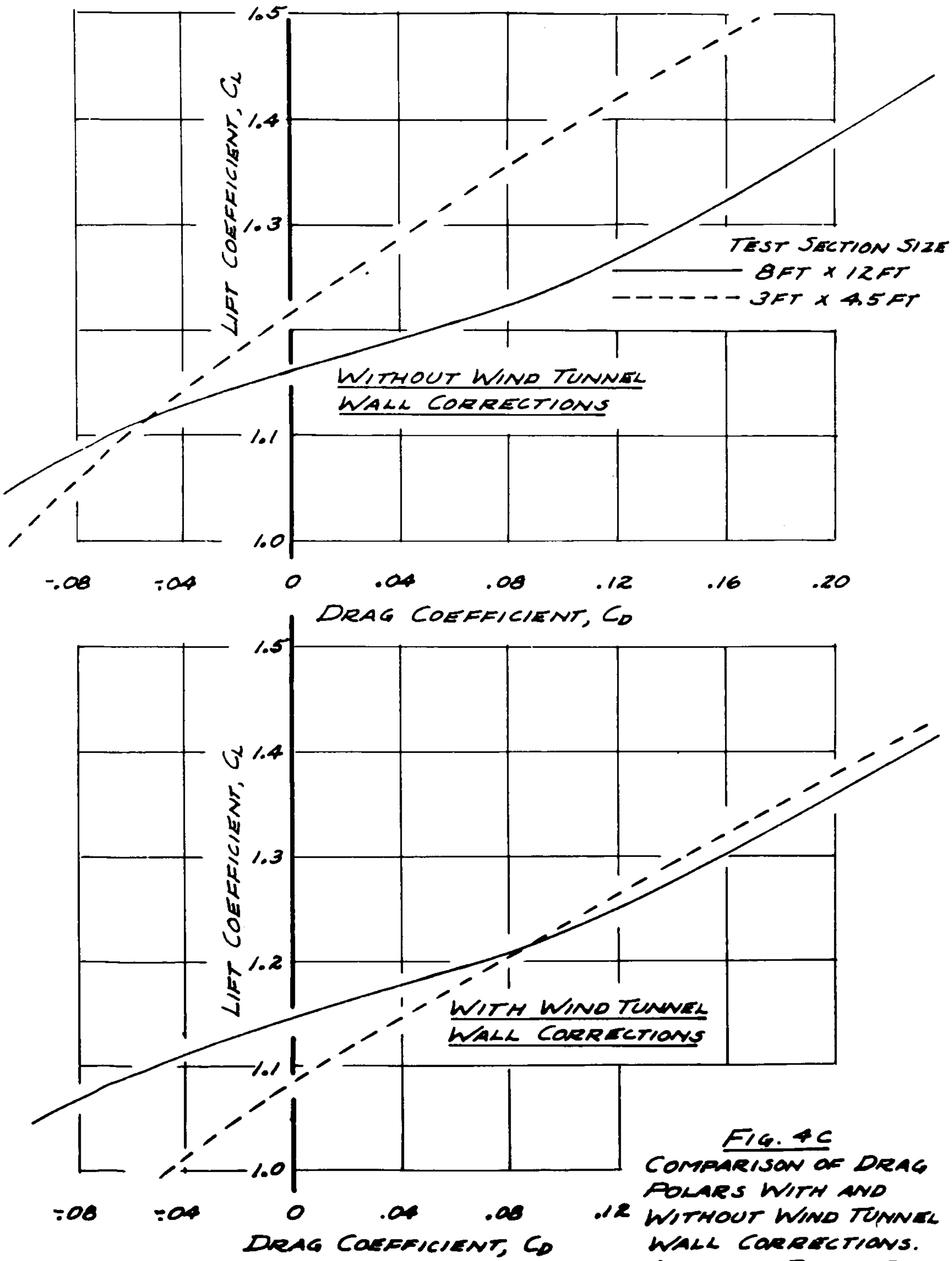

FIG. 4C
COMPARISON OF DRAG POLARS WITH AND WITHOUT WIND TUNNEL WALL CORRECTIONS.
ADVANCE RATIO, 0.10
BLADE ANGLE, +1.9°

D-415

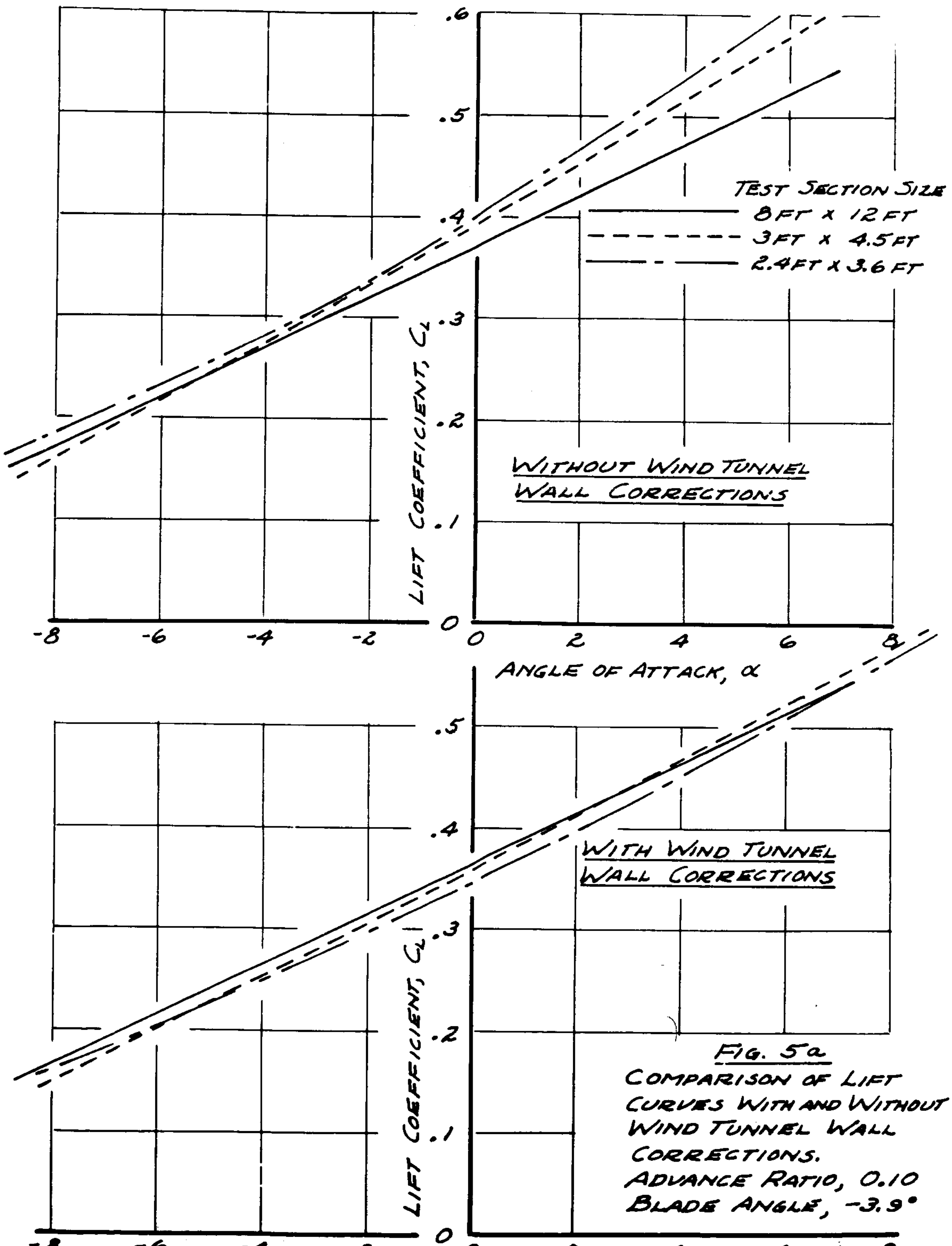

FIG. 5a
COMPARISON OF LIFT CURVES WITH AND WITHOUT WIND TUNNEL WALL CORRECTIONS.
ADVANCE RATIO, 0.10
BLADE ANGLE, −3.9°

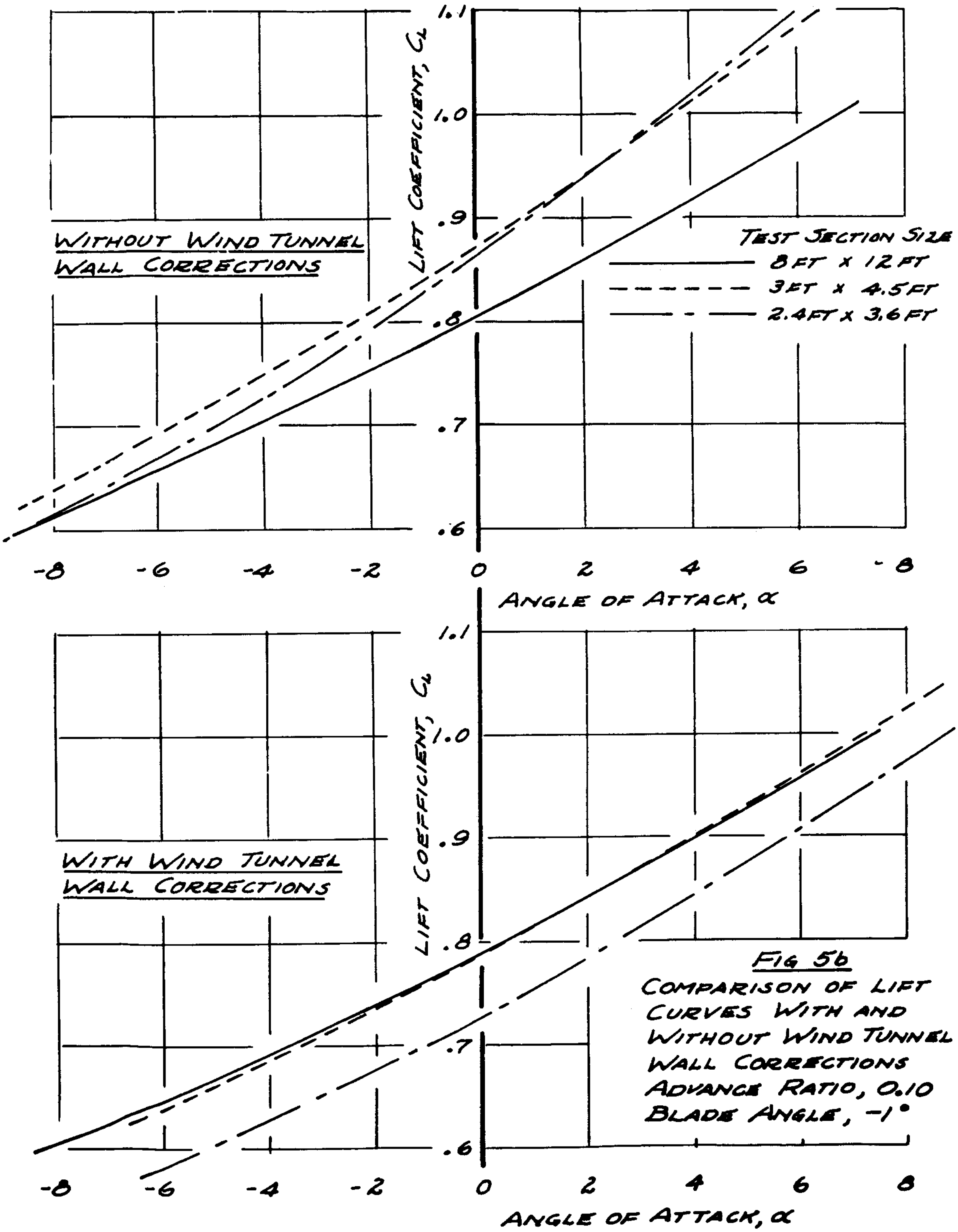

FIG 5b
COMPARISON OF LIFT CURVES WITH AND WITHOUT WIND TUNNEL WALL CORRECTIONS
ADVANCE RATIO, 0.10
BLADE ANGLE, $-1°$

D-415

D-415

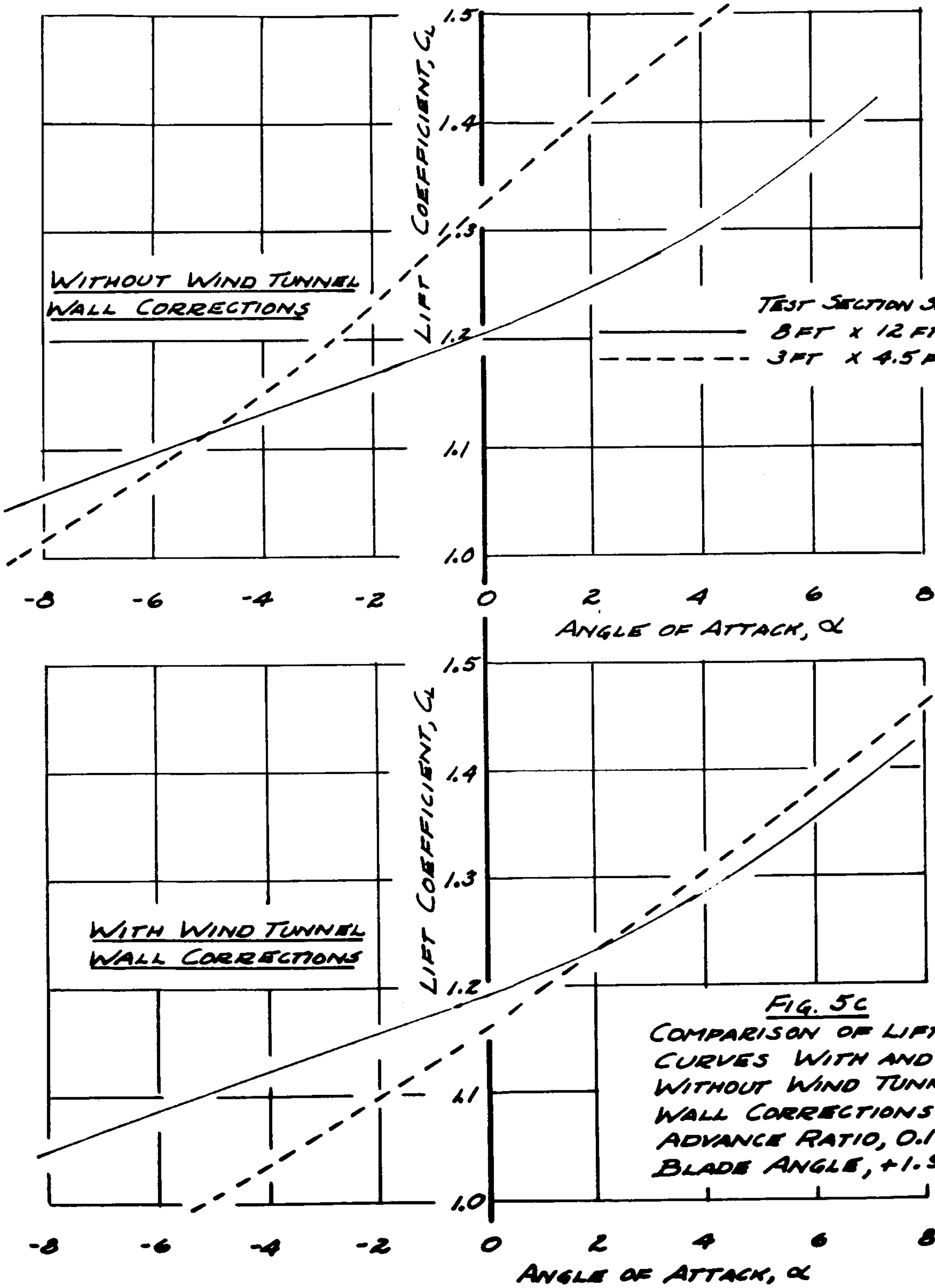

FIG. 5c
COMPARISON OF LIFT CURVES WITH AND WITHOUT WIND TUNNEL WALL CORRECTIONS. ADVANCE RATIO, 0.10 BLADE ANGLE, +1.9°

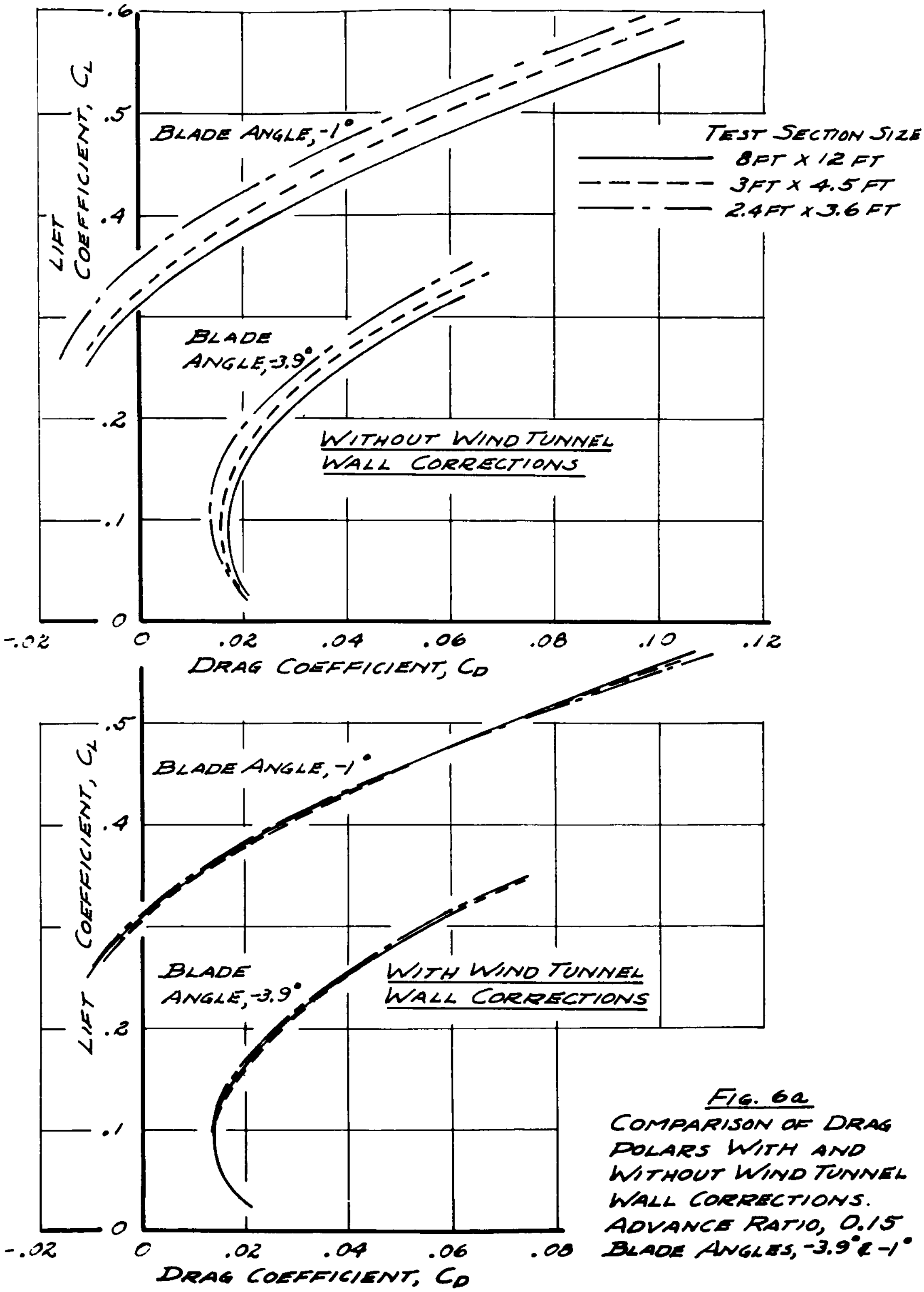

FIG. 6a

COMPARISON OF DRAG POLARS WITH AND WITHOUT WIND TUNNEL WALL CORRECTIONS. ADVANCE RATIO, 0.15 BLADE ANGLES, -3.9° & -1°

D-415

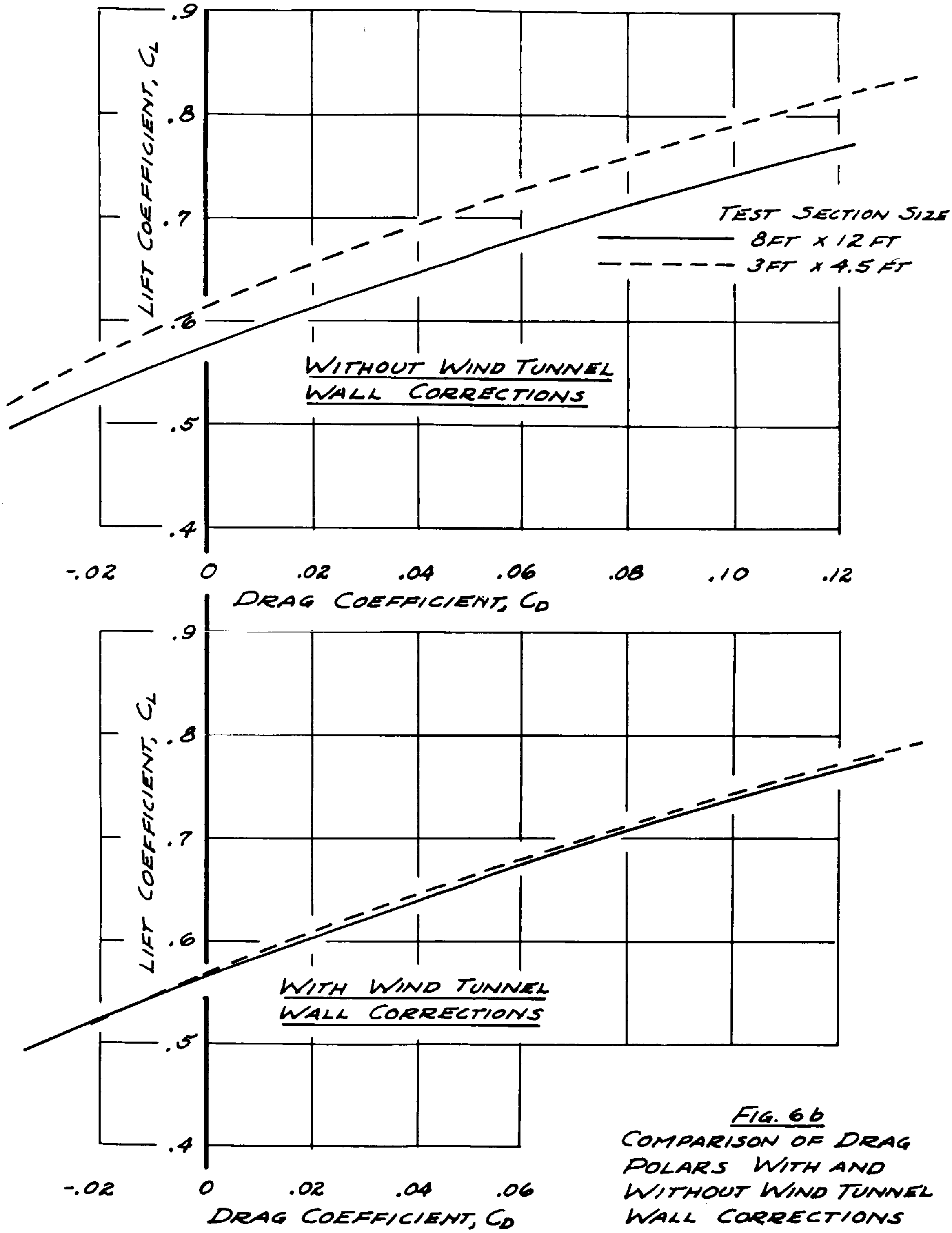

FIG. 6b
COMPARISON OF DRAG POLARS WITH AND WITHOUT WIND TUNNEL WALL CORRECTIONS
ADVANCE RATIO, 0.15
BLADE ANGLE, 1.9°

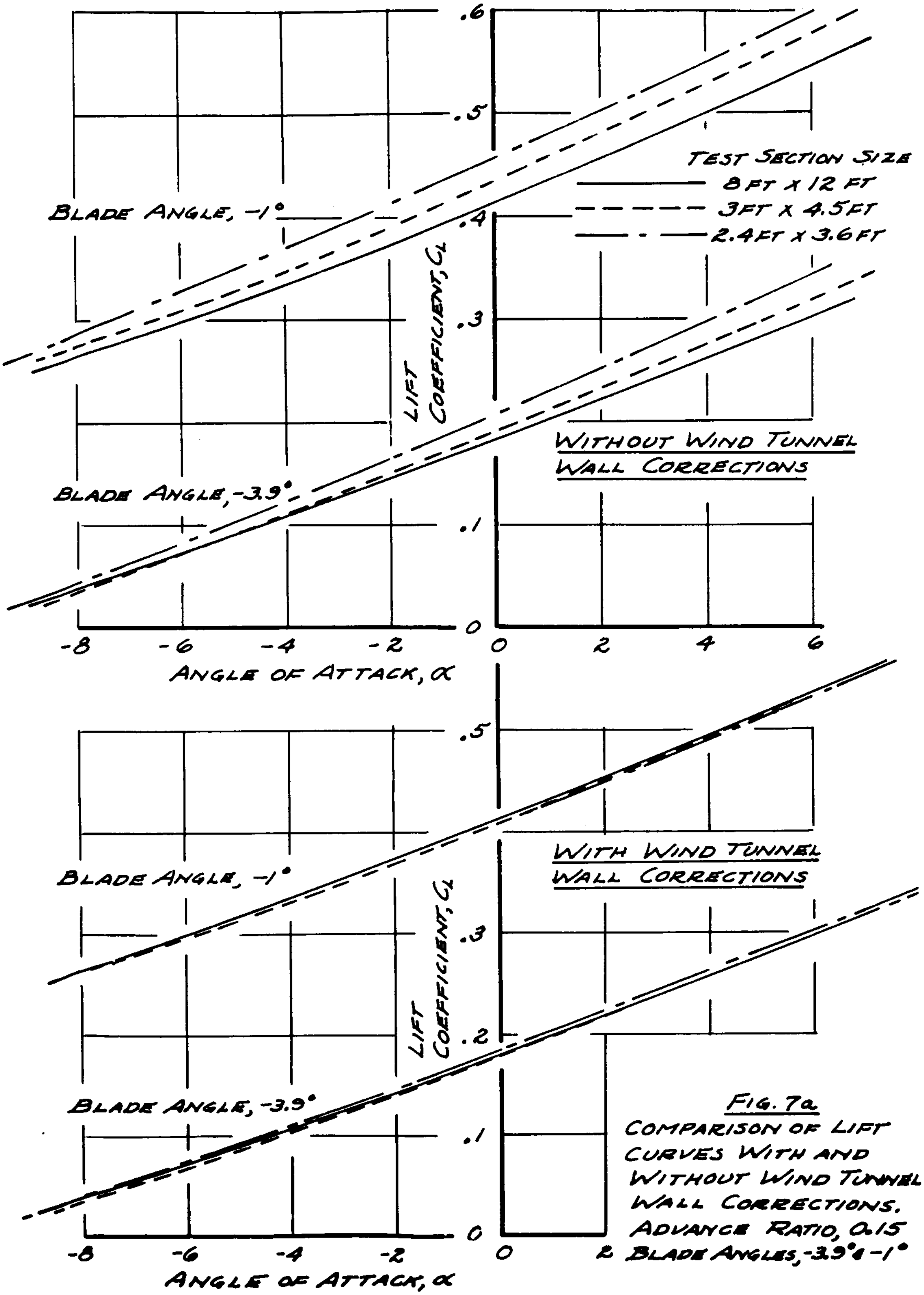

FIG. 7a
COMPARISON OF LIFT CURVES WITH AND WITHOUT WIND TUNNEL WALL CORRECTIONS.
ADVANCE RATIO, 0.15
2 BLADE ANGLES, -3.9° & -1°

D-415

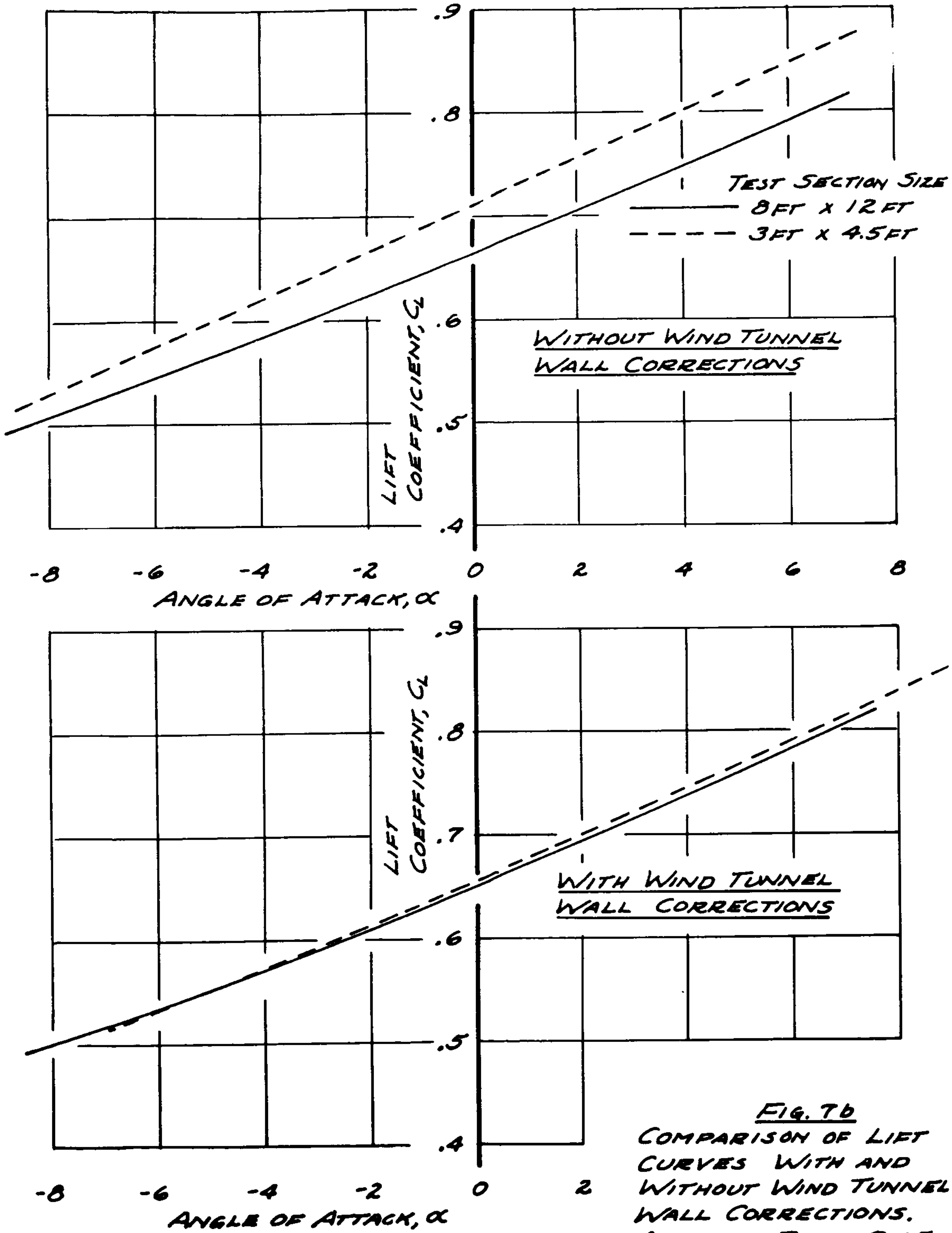

FIG. 7b
COMPARISON OF LIFT CURVES WITH AND WITHOUT WIND TUNNEL WALL CORRECTIONS.
ADVANCE RATIO, 0.15
BLADE ANGLE, 1.9°

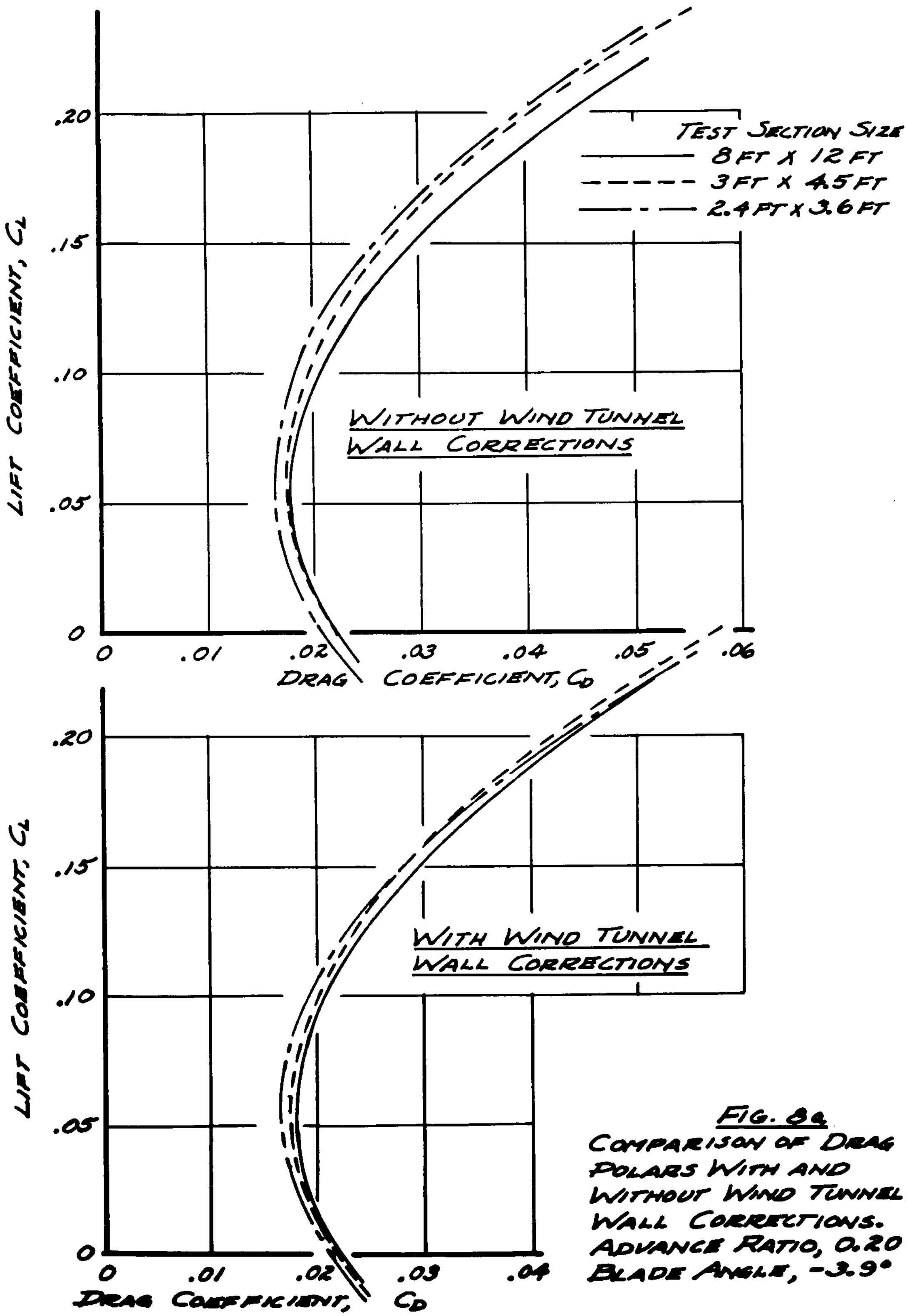

FIG. 8a
COMPARISON OF DRAG POLARS WITH AND WITHOUT WIND TUNNEL WALL CORRECTIONS. ADVANCE RATIO, 0.20 BLADE ANGLE, -3.9°

D-415

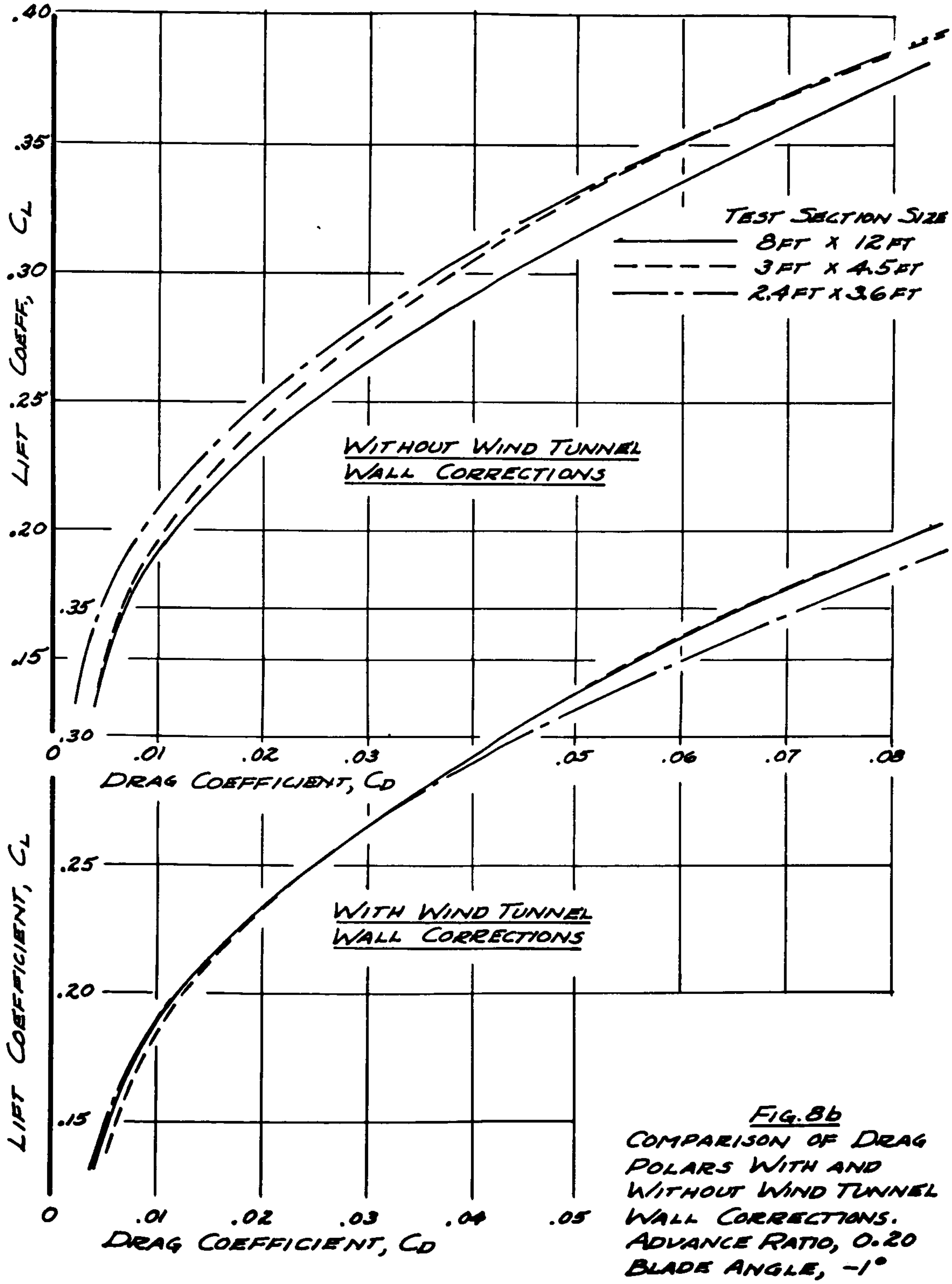

FIG. 8b
COMPARISON OF DRAG POLARS WITH AND WITHOUT WIND TUNNEL WALL CORRECTIONS. ADVANCE RATIO, 0.20 BLADE ANGLE, -1°

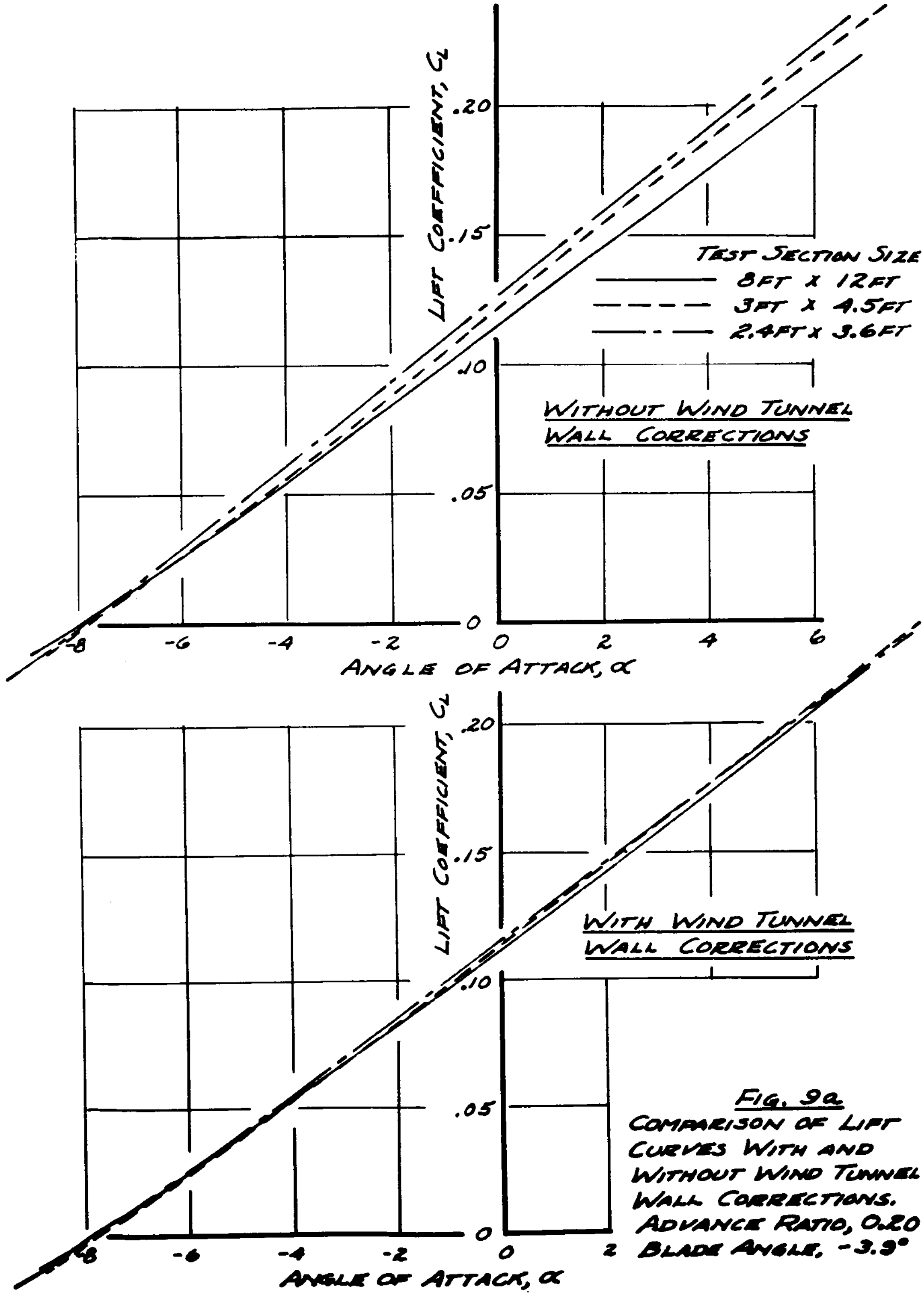

FIG. 9a

COMPARISON OF LIFT CURVES WITH AND WITHOUT WIND TUNNEL WALL CORRECTIONS. ADVANCE RATIO, 0.20 BLADE ANGLE, -3.9°

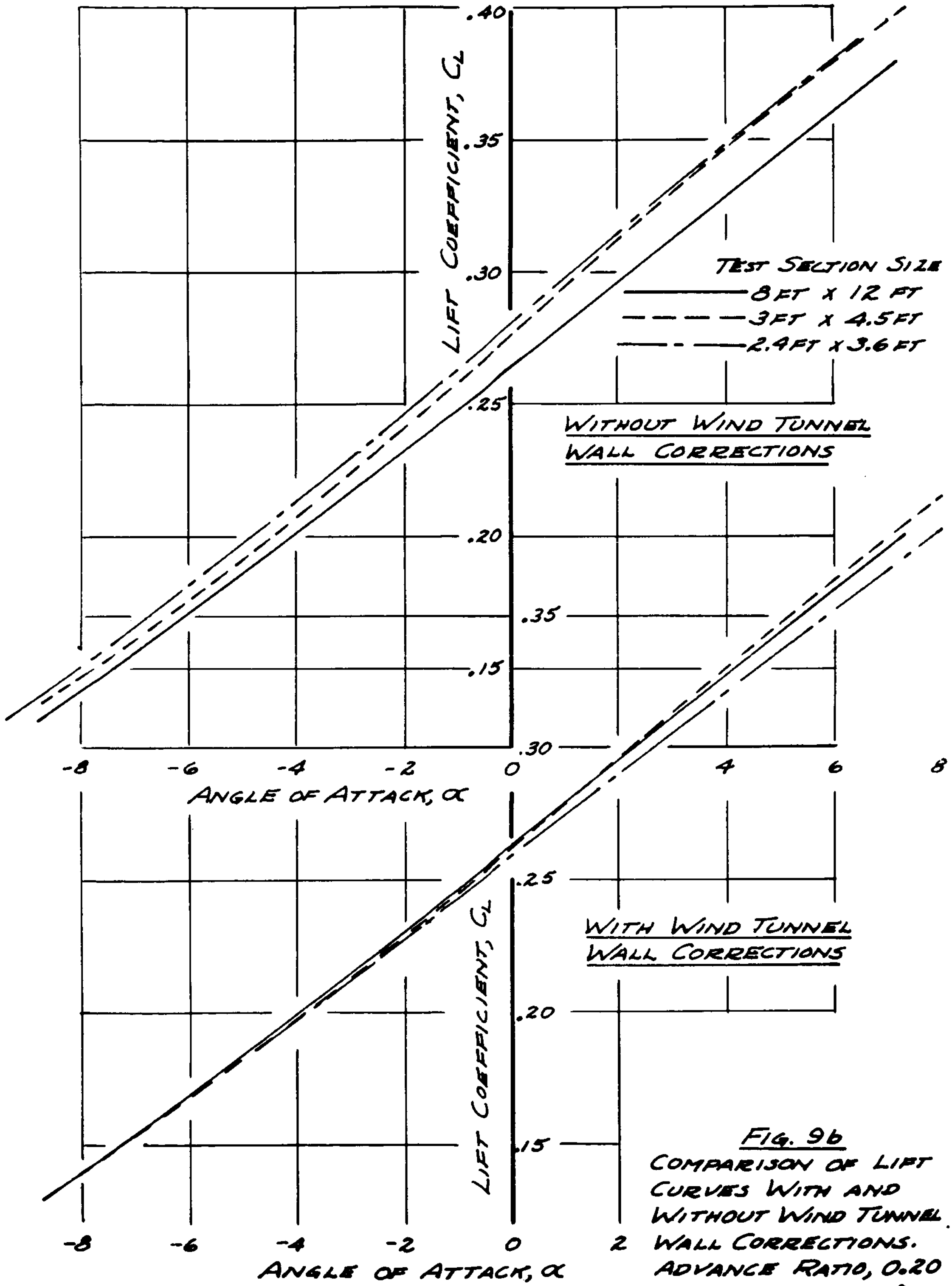

FIG. 9b
COMPARISON OF LIFT CURVES WITH AND WITHOUT WIND TUNNEL WALL CORRECTIONS.
ADVANCE RATIO, 0.20
BLADE ANGLE, -1°

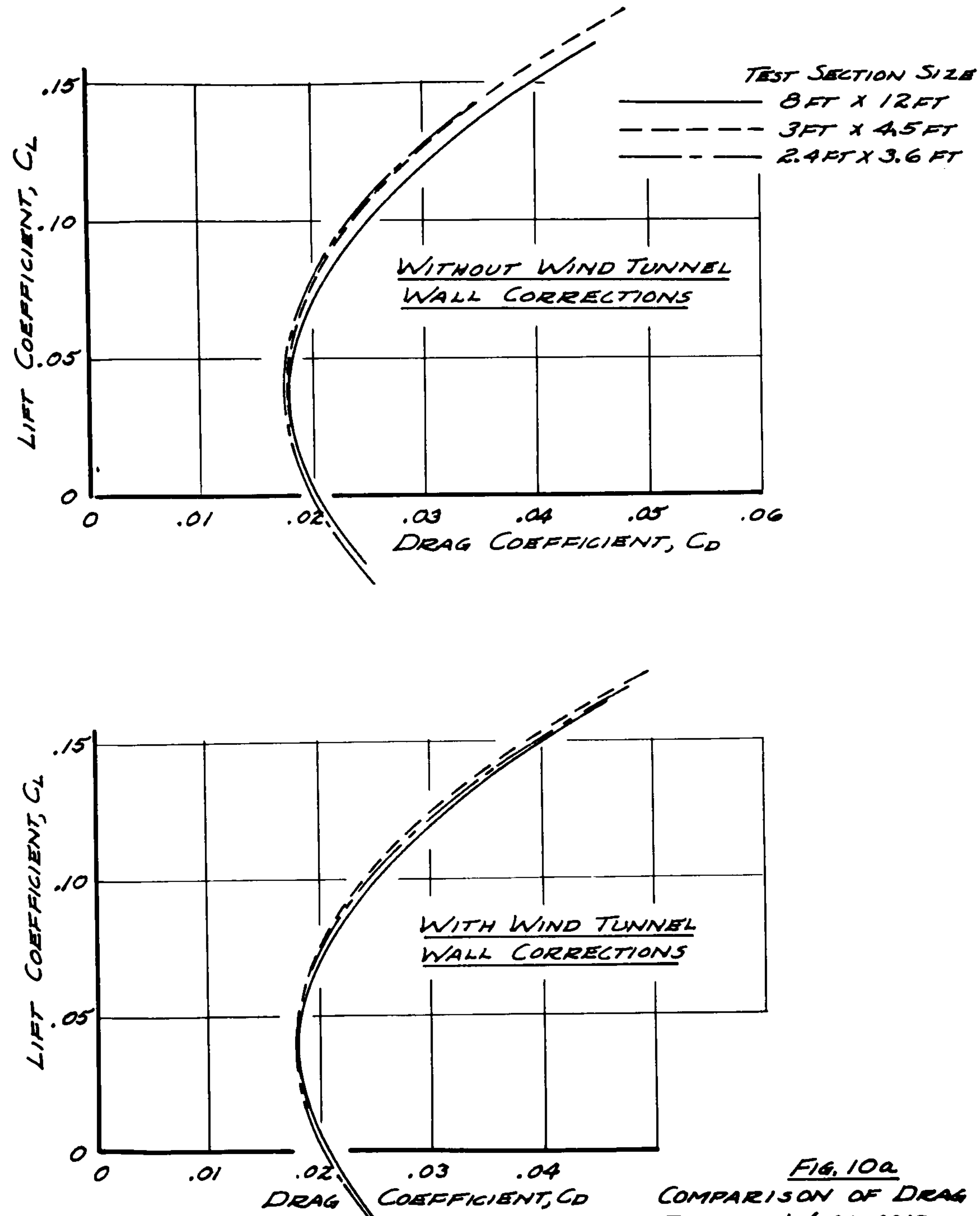

FIG. 10a

COMPARISON OF DRAG POLARS WITH AND WITHOUT WIND TUNNEL WALL CORRECTIONS.
ADVANCE RATIO, 0.25
BLADE ANGLE, −3.9°

D-415

D-415

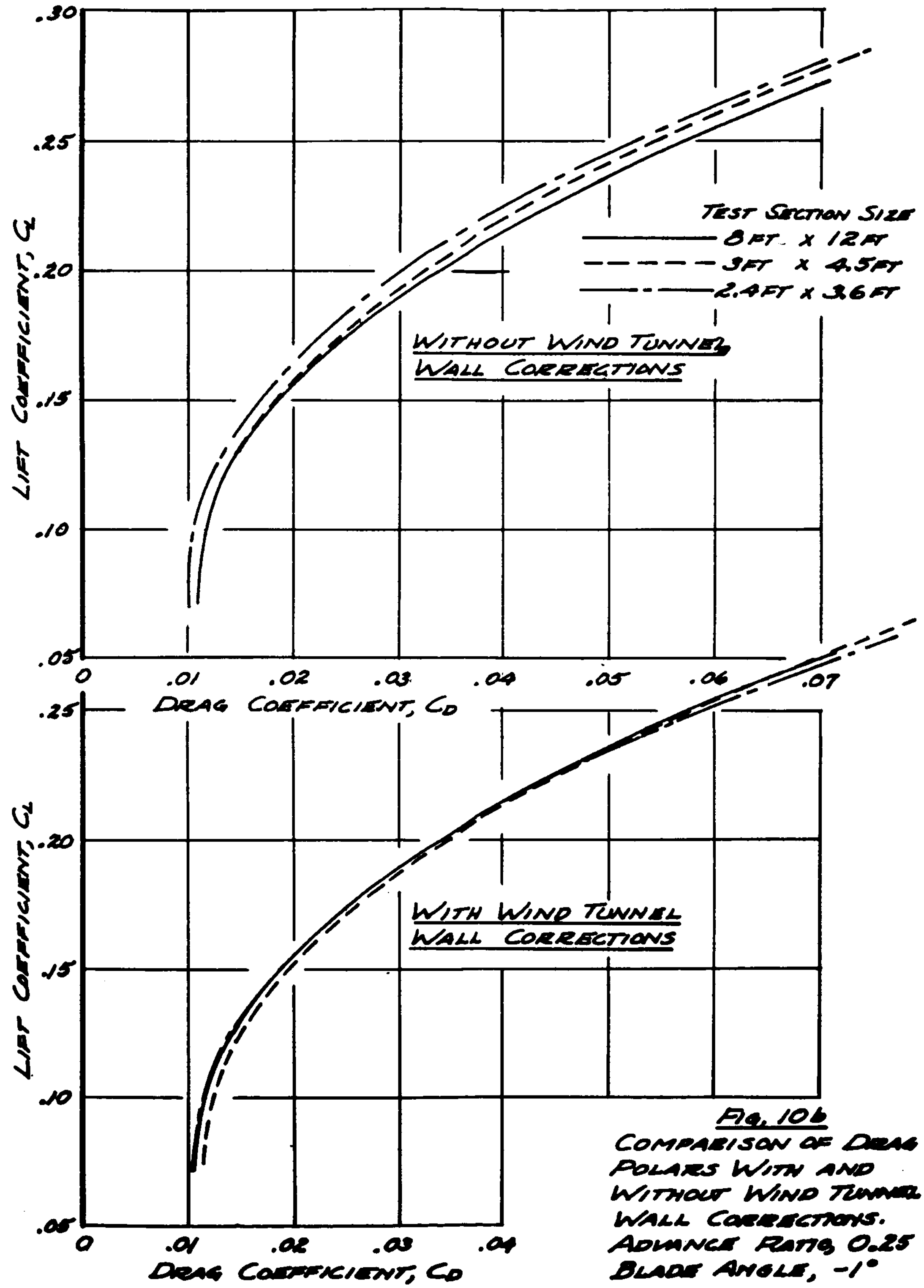

Fig. 10b
COMPARISON OF DRAG POLARS WITH AND WITHOUT WIND TUNNEL WALL CORRECTIONS.
ADVANCE RATIO, 0.25
BLADE ANGLE, -1°

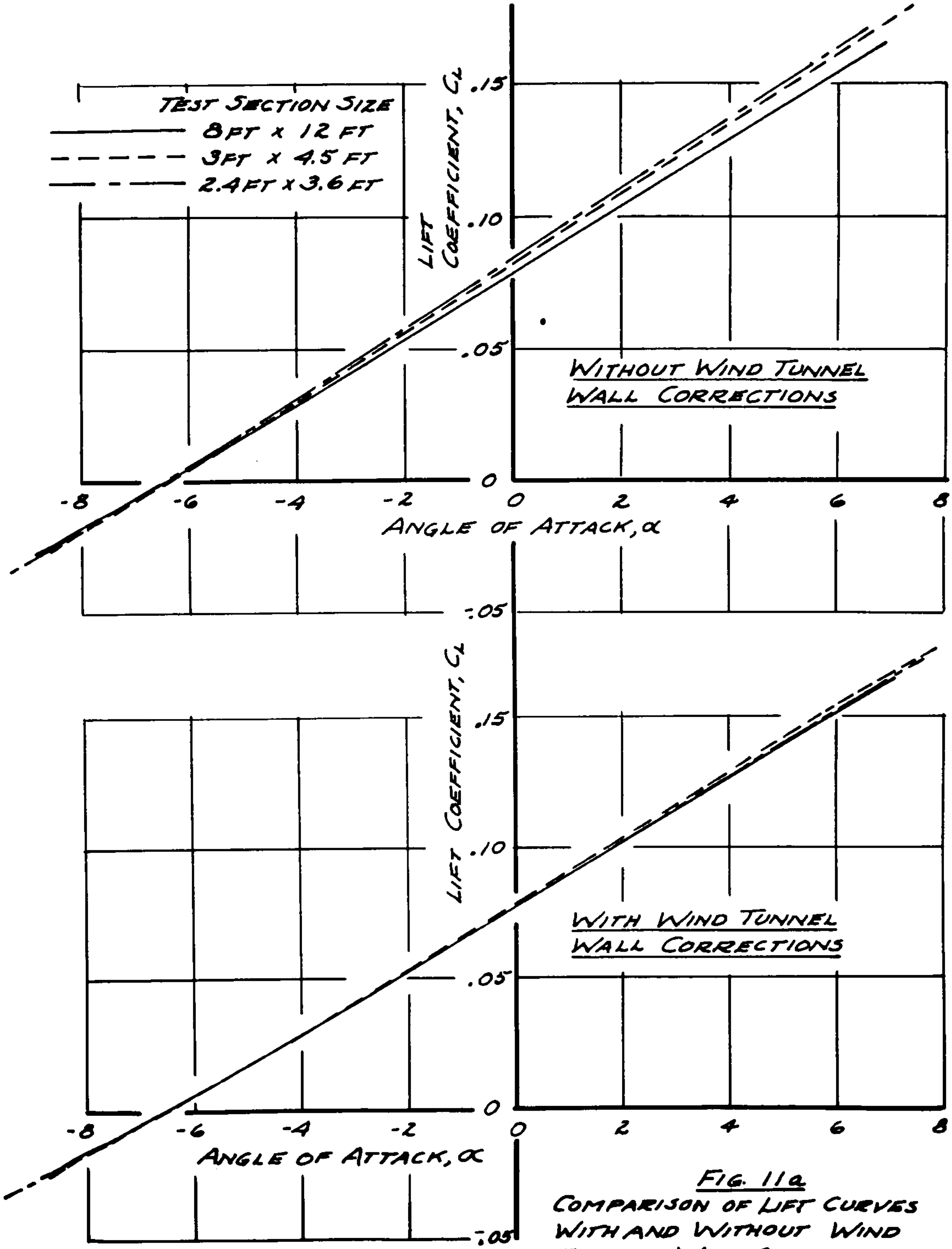

FIG. 11a
COMPARISON OF LIFT CURVES WITH AND WITHOUT WIND TUNNEL WALL CORRECTIONS
ADVANCE RATIO, 0.25
BLADE ANGLE, -3.9°

D-415

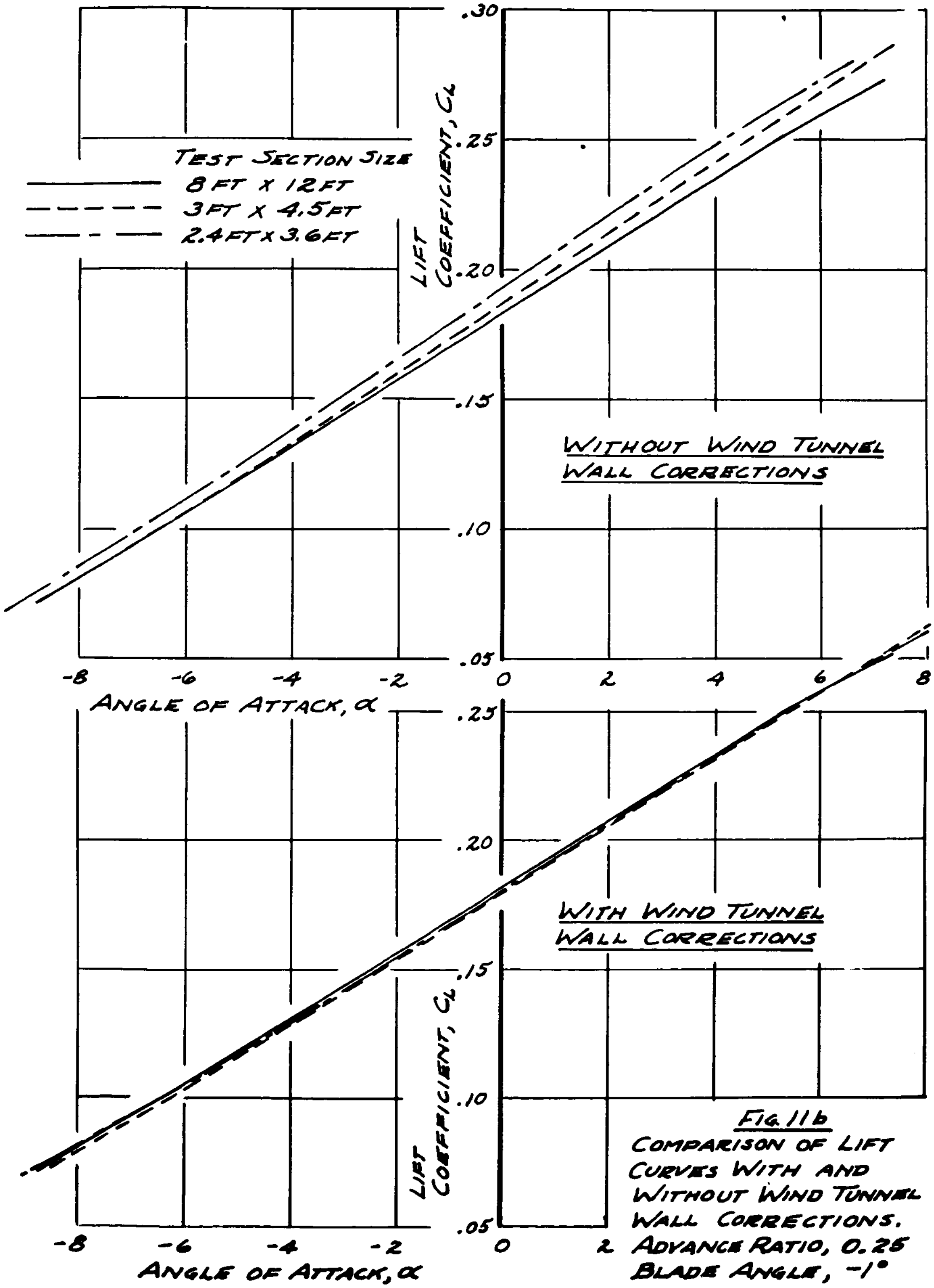

FIG. 11b
COMPARISON OF LIFT CURVES WITH AND WITHOUT WIND TUNNEL WALL CORRECTIONS.
ADVANCE RATIO, 0.25
BLADE ANGLE, $-1°$

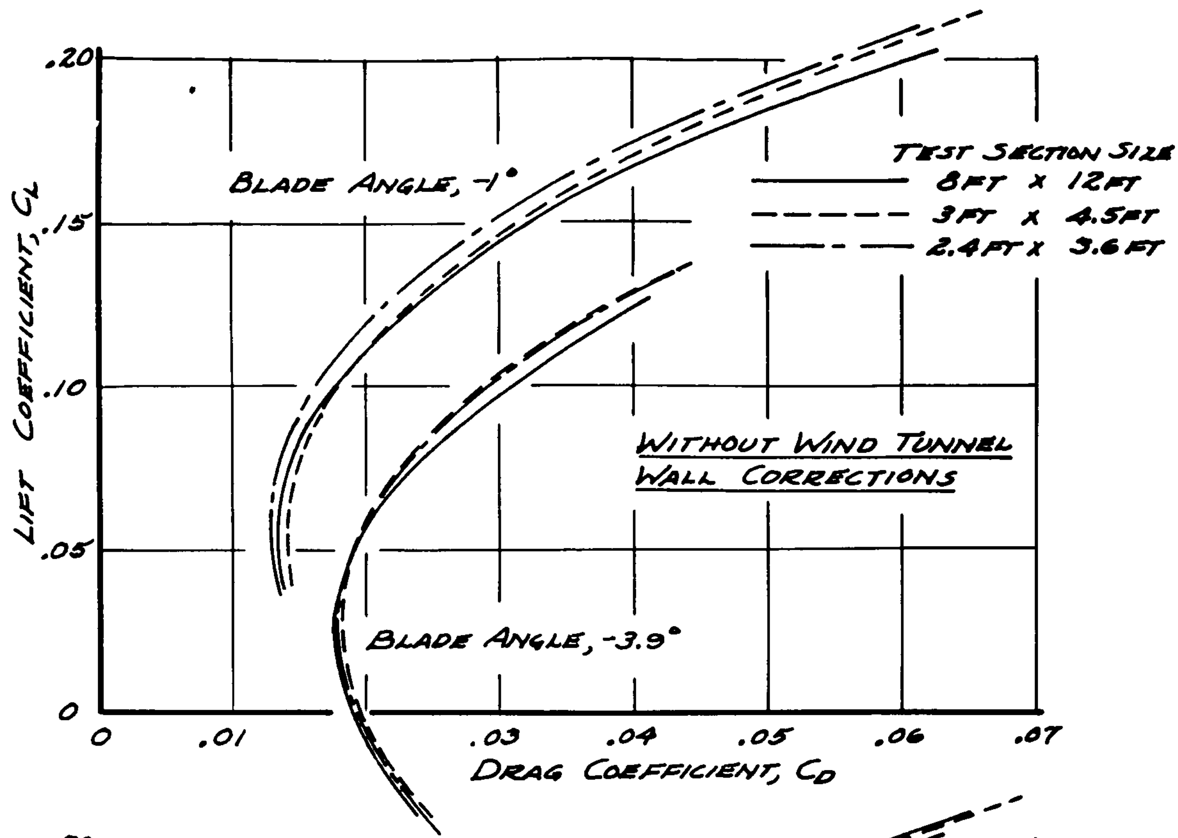

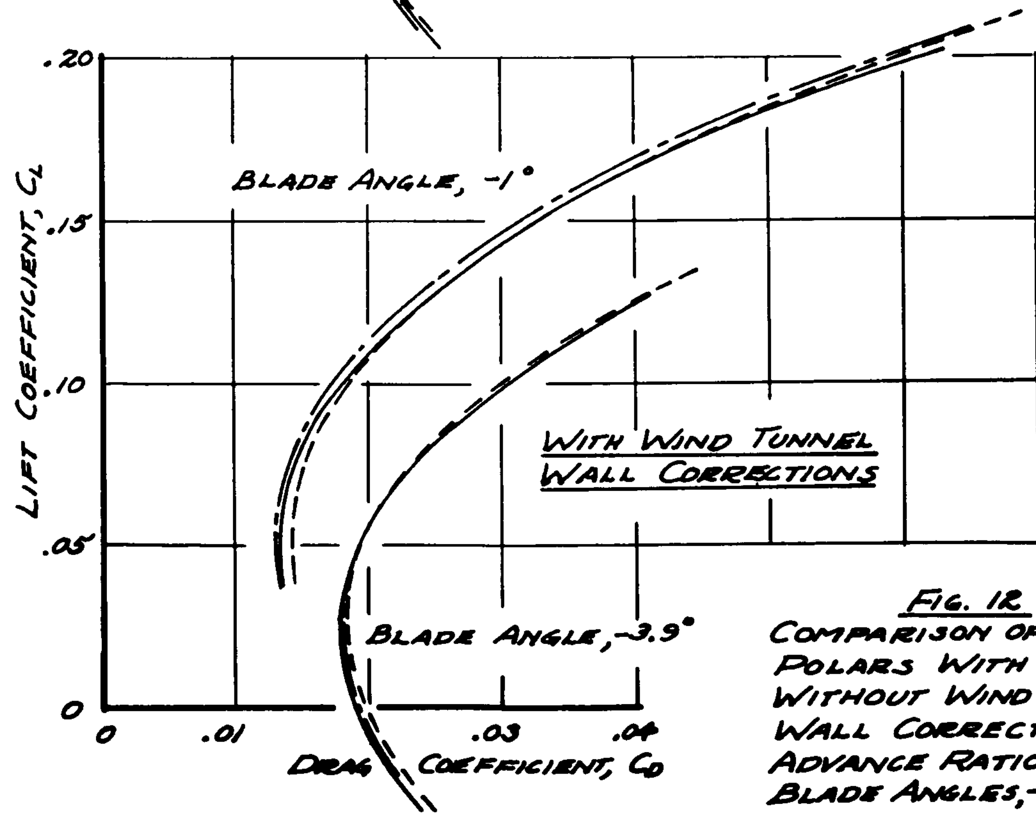

FIG. 12
COMPARISON OF DRAG POLARS WITH AND WITHOUT WIND TUNNEL WALL CORRECTIONS.
ADVANCE RATIO, 0.30
BLADE ANGLES, -3.9° & -1°

D-415

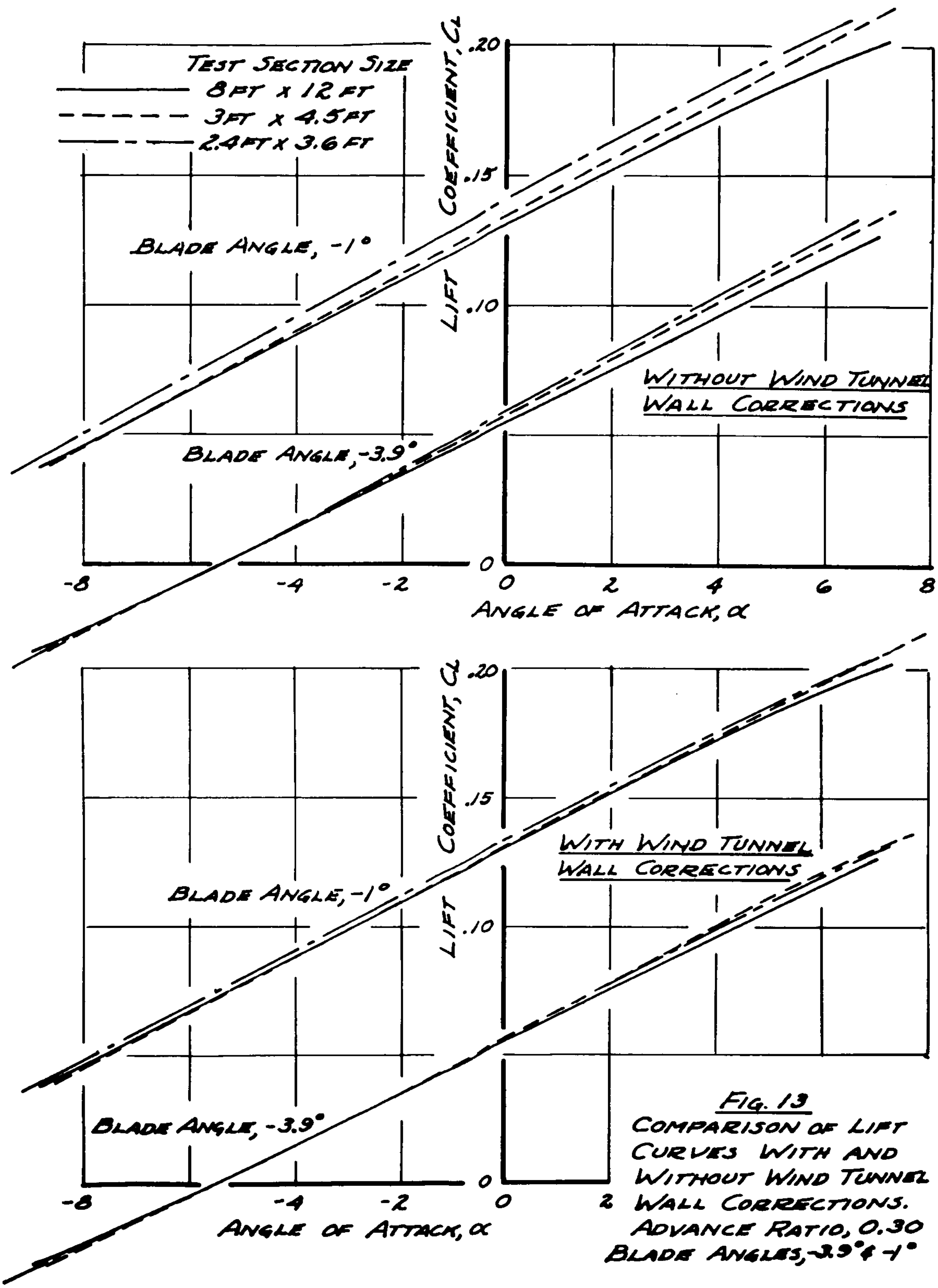

Fig. 13
Comparison of Lift Curves With and Without Wind Tunnel Wall Corrections. Advance Ratio, 0.30 Blade Angles, -3.9° & -1°